JACS
JOURNAL OF THE AMERICAN CHEMICAL SOCIETY
Article
pubs.acs.org/JACS

Radically Enhanced Molecular Switches

Albert C. Fahrenbach,[†,§] Zhixue Zhu,[†] Dennis Cao,[†,§] Wei-Guang Liu,[⊥] Hao Li,[†] Sanjeev K. Dey,[†] Subhadeep Basu,[†] Ali Trabolsi,[†,∥] Youssry Y. Botros,[‡,#,▽] William A. Goddard, III,[§,⊥] and J. Fraser Stoddart*[,†,§]

[†]Department of Chemistry and [‡]Department of Materials Science, Northwestern University 2145 Sheridan Road, Evanston, Illinois 60208, United States

[§]NanoCentury KAIST Institute and Graduate School of EEWS (WCU), Korea Advanced Institute of Science and Technology (KAIST), 373-1 Guseong Dong, Yuseong Gu, Daejeon 305-701 Republic of Korea

[⊥]Materials and Process Simulation Center, California Institute of Technology, Pasadena, California 91125, United States

[∥]Center for Science and Engineering, New York University Abu Dhabi, Abu Dhabi, United Arab Emirates

[#]Intel Laboratories, Building RNB-6-61, 2200 Mission College Blvd., Santa Clara, California 95054-1549, United States

[▽]National Center for Nano Technology Research, King Abdulaziz City for Science and Technology, P.O. Box 6086, Riyadh 11442, Kingdom of Saudi Arabia

Supporting Information

ABSTRACT: The mechanism governing the redox-stimulated switching behavior of a tristable [2]rotaxane consisting of a cyclobis(paraquat-*p*-phenylene) ($CBPQT^{4+}$) ring encircling a dumbbell, containing tetrathiafulvalene (TTF) and 1,5-dioxynaphthalene (DNP) recognition units which are separated from each other along a polyether chain carrying 2,6-diisopropylphenyl stoppers by a 4,4′-bipyridinium ($BIPY^{2+}$) unit, is described. The $BIPY^{2+}$ unit acts to increase the lifetime of the metastable state coconformation (MSCC) significantly by restricting the shuttling motion of the $CBPQT^{4+}$ ring to such an extent that the MSCC can be isolated in the solid state and is stable for weeks on end. As controls, the redox-induced mechanism of switching of two bistable [2]rotaxanes and one bistable [2]catenane composed of $CBPQT^{4+}$ rings encircling dumbbells or macrocyclic polyethers, respectively, that contain a $BIPY^{2+}$ unit with either a TTF or DNP unit, is investigated. Variable scan-rate cyclic voltammetry and digital simulations of the tristable and bistable [2]rotaxanes and [2]catenane reveal a mechanism which involves a bisradical state coconformation (BRCC) in which only one of the $BIPY^{\bullet+}$ units in the $CBPQT^{2(\bullet+)}$ ring is oxidized to the $BIPY^{2+}$ dication. This observation of the BRCC was further confirmed by theoretical calculations as well as by X-ray crystallography of the [2]catenane in its bisradical tetracationic redox state. It is evident that the incorporation of a kinetic barrier between the donor recognition units in the tristable [2]rotaxane can prolong the lifetime and stability of the MSCC, an observation which augurs well for the development of nonvolatile molecular flash memory devices.

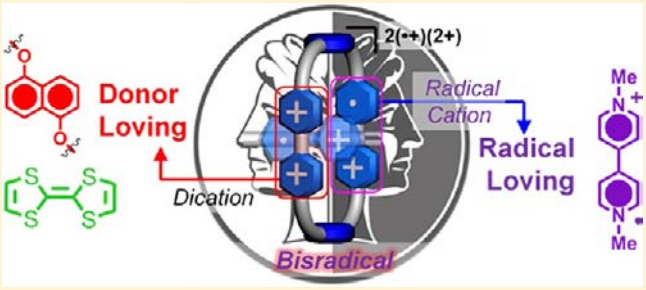

INTRODUCTION

The drive to achieve the miniaturization of electronic devices beyond the limits that "top-down" conventional lithographic techniques can provide has led[1] to the research and development of an array of "bottom-up" protocols. One approach invented and implemented by Hawker et al.[2] relies on the use of nanoscale lithographic templates made possible by the self-assembly of block copolymers into highly ordered hexagonal and rectilinear arrays. Another approach created and developed by Mirkin et al.[3] relies on the use of atomic force microscopy (AFM) tips within the context of what has become known as dip-pen nanolithography (DPN), which when used as massively parallel arrays of "ink"-coated tips can deliver soft organic substrates onto hard surfaces with remarkable degrees of order and complexity. In the realm of molecular electronics,[4] where the objective very often is to understand the electronic behavior of single molecules bridging the gap between two electrodes, some extraordinary advances have been made[5] in recent years. For example, Fujita et al.[5b] have demonstrated the use of self-assembled nanocages in between a gold substrate and a scanning tunneling microscopy (STM) tip, which act as hosts for a relatively small number of π-stacked organic guests. By controlling the size of the cage, the researchers were able to investigate the conductance of single discrete stacks of two, three, and four π-electron-deficient anthracene-type moieties in a very precise manner. In collaboration with Heath,[6] we have relied on fabrication of nanoelectronic devices with two-

Received: June 20, 2012
Published: September 24, 2012

   dx.doi.org/10.1021/ja306044r | J. Am. Chem. Soc. 2012, 134, 16275−16288

dimensional "cross-bar" architectures, employing a superlattice nanowire pattern transfer[7] (SNAP) methodology, in which bistable [2]rotaxane[8] molecules by the hundreds or thousands are sandwiched as molecular monolayers between the top and bottom crossbar elements in a molecular switch tunnel junction (MSTJ). These bistable rotaxanes served as the active binary components[6f] of this molecular memory device. This device has demonstrated[6f] data density storage capacity predicted at the time (2007) by Moore's Law not to become available until at least the year 2020.

The bistable [2]rotaxanes that were incorporated into these memory devices were those whose redox-active switching is achieved by employing the π-electron-poor tetracationic cyclophane, cyclobis(paraquat-*p*-phenylene)[9] ($CBPQT^{4+}$), mechanically interlocked around a dumbbell component incorporating π-electron-rich 1,5-dioxynaphthalene (DNP) and redox-active tetrathiafulvalene[10] (TTF) units. The $CBPQT^{4+}$ ring encircles the TTF unit predominantly in the ground state of such bistable [2]rotaxanes at equilibrium, leading to the naming[11] of this translational isomer as the ground-state coconformation (GSCC). The ring can be made to encircle the DNP unit, as a result of an oxidation/reduction cycle of TTF, to form a translational isomer known as the metastable-state coconformation[11] (MSCC). The fact that the MSCC represents a higher conductive state than the GSCC was exploited[6f] to achieve single bits of memory in the context of the device, i.e., the GSCC represents a "0" and the MSCC represents a "1" for a collection of these bistable [2]rotaxanes possessing these particular states in monolayers trapped within an array of MSTJs. The memory implanted in these devices is volatile, however, and only lasts[6f] for about an hour. One of the hypotheses which attempts to rationalize the volatile nature of these molecular memory devices is one that reasons that the relaxation of the MSCC back to the GSCC also occurs after about an hour within the MSTJ environment. Therefore, developing a strategy to increase the lifetime of the MSCC provides a means of testing this hypothesis, and also holds out the prospect of being able to construct nonvolatile molecular memory devices.

A strategy which has undergone significant scrutiny in order to increase the lifetime of the MSCC has been one focused on inserting kinetic barriers[12] between the TTF and DNP units that would act to slow down the shuttling motion of the $CBPQT^{4+}$ ring, trapping the MSCC kinetically once it is populated. Such kinetic barriers or "speed bumps" have included steric ones,[13] such as *trans*-azobenzene[13e,g] units or even foldamers.[13f] Another strategy employs the use of electrostatic barriers,[14] such as 4,4′-bipyridinium dicationic ($BIPY^{2+}$) units,[15] which, on account of Coulombic repulsion with the $CBPQT^{4+}$ ring, have also been shown[14c−e] to increase the lifetime of the MSCC. Furthermore, once we have a way of trapping the MSCC, we must also have the means of releasing it in a timely manner. Such a capability would provide an erase mechanism in the context of molecular memory devices, allowing for the development[16] of bistable rotaxane-based molecular flash memory.

Herein, we describe a detailed mechanistic investigation of the redox-active switching behavior of a [2]rotaxane $\mathbf{R3}^{6+}$ (Scheme 1) composed of the $CBPQT^{4+}$ ring, mechanically interlocked with a dumbbell component containing a $BIPY^{2+}$ unit flanked on each side by a TTF and a DNP unit. This investigation is supported by study of its related [2]rotaxanes $\mathbf{R1}^{6+}$ and $\mathbf{R2}^{6+}$, wherein, respectively, either TTF or DNP is absent from the dumbbell component along with a bistable [2]catenane $\mathbf{C1}^{6+}$ incorporating a macrocyclic polyether which contains DNP and $BIPY^{2+}$ units. We show that the $BIPY^{2+}$ unit in $\mathbf{R3}^{6+}$ serves as such an effective electrostatic barrier that it is possible to employ a synthetic procedure for trapping and isolating the MSCC as a pure solid. In particular, we report the reduction-induced switching that makes use of favorable radical−radical interactions,[17] which occur between $BIPY^{\bullet+}$ radical cations in the ring and dumbbell/macrocycle components in these mechanically interlocked molecules (MIMs), using variable temperature and variable scan-rate cyclic voltammetry (CV) in combination with digital simulations and X-ray crystallography. Moreover, we show by variable scan-rate CV as well as by UV−vis and ^{1}H NMR spectroscopies that we can employ the dynamic nature of these radical−radical interactions to restore the GSCC from the kinetically trapped MSCC. Such a demonstration also outlines a strategy[18] for gaining a large degree of control over the relative mechanical motions of the components within a switchable MIM that relies on only *one* type of stimulus, i.e., redox chemistry.

Scheme 1. Structural Formulas and Graphical Representations of the [2]Catenane $\mathbf{C1}^{6+}$ Containing a Macrocyclic Polyether with DNP and $BIPY^{2+}$ Units, the [2]Rotaxane $\mathbf{R1}^{6+}$ Incorporating DNP and $BIPY^{2+}$ Units, the [2]Rotaxane $\mathbf{R2}^{6+}$ Incorporating TTF and $BIPY^{2+}$ Units, and the Tristable [2]Rotaxane $\mathbf{R3}^{6+}$ Incorporating DNP, TTF, and $BIPY^{2+}$ Units[a]

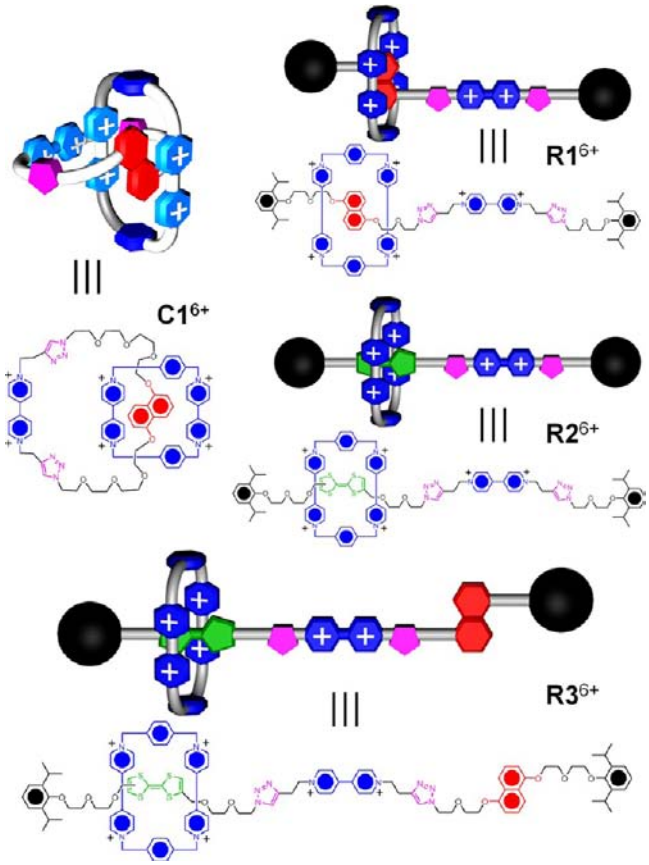

[a]All compounds were studied as their hexafluorophosphate salts.

Design Considerations. In a previous publication, we described[17h] the synthesis of the tristable [2]rotaxane $\mathbf{R3}^{6+}$

dx.doi.org/10.1021/ja306044r | J. Am. Chem. Soc. 2012, 134, 16275−16288

(Scheme 1), which can be switched electrochemically between three thermodynamic states that alter the translational position of the ring. Upon oxidation of the TTF unit, the $CBPQT^{4+}$ ring is obliged to translate over the $BIPY^{2+}$ unit in order to encircle the DNP unit, in a pathway which is activated[19] by Coulombic energy. This Coulombic repulsion between the $CBPQT^{4+}$ ring and $TTF^{\bullet+/2+}$ unit is what enables the ring to pass over the $BIPY^{2+}$ electrostatic barrier rapidly, in a process which we hypothesize,[20] based on theoretical calculations, proceeds at a rate of approximately 10^8 s^{-1}. We have also demonstrated[11c,14c] beforehand that thermal relaxation of the MSCC to the GSCC, that is, translation of the $CBPQT^{4+}$ ring from the DNP unit over the $BIPY^{2+}$ electrostatic barrier and onto the TTF unit, occurs at a rate governed by a free energy barrier[21] of 19 kcal mol^{-1}. The rate of relaxation is decreased[14c] 100-fold as a consequence of the presence of the $BIPY^{2+}$ unit; therefore, we have defined (Scheme 2) the coconformation in which the $CBPQT^{4+}$ ring is positioned over the $BIPY^{2+}$ unit as the transition-state coconformation (TSCC) and, as the name implies, is not actually a thermodynamically stable state yet is a coconformation that must be considered in order for shuttling of the $CBPQT^{4+}$ ring to occur. The notion of the TSCC is a mechanistic feature which is necessary to consider when discussing (*vide infra*) the reduction-based mechanism of switching in all the MIMs.

Scheme 2. Generalized Graphical Representations of the Assigned Coconformations for the Trisradical, Bisradical and Fully-Oxidized Electronic States[a]

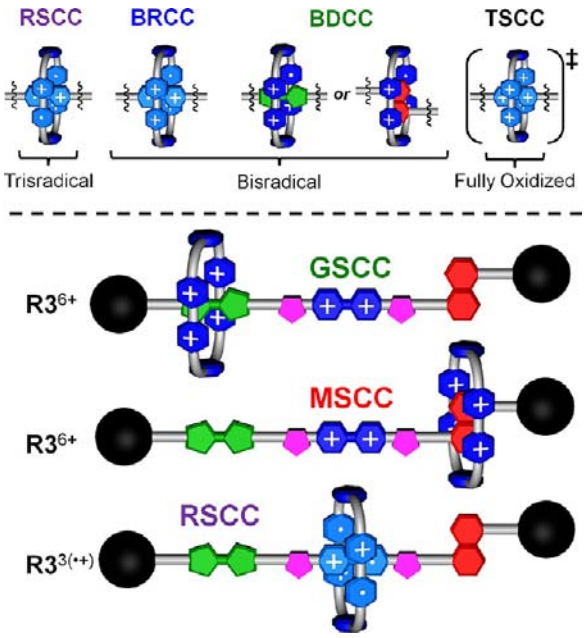

[a]In the case of the tristable rotaxane $\mathbf{R3}^{6+}$, the ground redox state can exist in three forms, as the thermodynamically stable GSCC, the MSCC, and the activated TSCC. The bisradical oxidation state has two forms, namely, the BRCC and the BDCC. It is important to note that, in the BDCC, one of the radicals is located on the $CBPQT^{(\bullet+)(2+)}$ ring, while the other is still associated with the $BIPY^{\bullet+}$ unit in the dumbbell or macrocycle component, which are not shown. The trisradical state is only observed to have one form, defined as the RSCC. Shown below are specific examples of the rotaxane $\mathbf{R3}^{6+}$ in its GSCC and MSCC and once reduced to its trisradical form, its RSCC.

In relation to the ability of the rotaxane $\mathbf{R3}^{6+}$ to switch by virtue of $BIPY^{\bullet+}$ radical–radical interactions, we have shown[17h–j] previously that upon a three-electron reduction in which two electrons are transferred to the $CBPQT^{4+}$ ring and one to the $BIPY^{2+}$ unit of the dumbbell, the resulting $CBPQT^{2(\bullet+)}$ ring encircles the $BIPY^{\bullet+}$ radical cation as the most thermodynamically stable coconformation. We label (Scheme 2) this translational isomer as the radical-state coconformation (RSCC). The stability of this state comes about through favorable radical–radical interactions, referred to previously as "pimerization",[17c] that is, a process which occurs between two or more $BIPY^{\bullet+}$ radical cations. We reported[17j] recently a detailed investigation of the supramolecular properties during the formation of the trisradical complex which occurs spontaneously between the $CBPQT^{2(\bullet+)}$ ring and the methyl viologen radical cation, $MV^{\bullet+}$. In particular, the mechanism involves a bisradical intermediate $CBPQT^{(\bullet+)(2+)} \subset MV^{\bullet+}$ en route to reoxidation of the trisradical complex to its fully oxidized form. This bisradical intermediate occurs as a consequence of spin-pairing to a singlet state, such that only two $BIPY^{\bullet+}$ radical cations of the complex are paired at any one time, rendering the third unpaired $BIPY^{\bullet+}$ easier to oxidize in relation to the other two. We demonstrate in this paper that a similar bisradical intermediate is involved in the switching mechanism of these MIMs. As a consequence of the fact that the $CBPQT^{(\bullet+)(2+)}$ ring component contains both $BIPY^{2+}$ and $BIPY^{\bullet+}$ units in the bisradical tetracationic redox state of these MIMs, the ring is both "donor-loving" and "radical-loving" at the same time. This dichotomy leads to the shuttling of the $CBPQT^{(\bullet+)(2+)}$ ring from the $BIPY^{\bullet+}$ radical cation unit to the π-electron-rich donor unit, i.e., TTF or DNP. We label the coconformation (Scheme 2) when the $CBPQT^{(\bullet+)(2+)}$ ring encircles the $BIPY^{\bullet+}$ radical cation as the bisradical state coconformation (BRCC). When the $CBPQT^{(\bullet+)(2+)}$ ring encircles either the TTF or DNP unit, we define it as the bisradical donor state coconformation (BDCC). This shuttling of the $CBPQT^{(2+)(\bullet+)}$ ring can be harnessed further in the case of the rotaxane $\mathbf{R3}^{6+}$ so as to remove the dependence involved in restoring the GSCC from the MSCC by means of a thermally activated pathway, by providing a redox-activated one. We now proceed in our discussion by first of all considering the mechanistic features of the simpler cases of the two [2]rotaxanes $\mathbf{R1}^{6+}$ and $\mathbf{R2}^{6+}$ as well as those of the [2]catenane $\mathbf{C1}^{6+}$.

RESULTS AND DISCUSSION

CV and Digital Simulations. *[2]Catenane* $\mathbf{C1}^{6+}$. The synthesis of the [2]catenane $\mathbf{C1}^{6+}$ was achieved using a previously reported[22] protocol. The electrochemical switching of the catenane $\mathbf{C1}^{6+}$ was investigated by variable scan-rate CV and compared to digital simulations generated from the proposed mechanism. At the slow scan rate of 20 mV s^{-1} (Figure 1a, purple trace), an initial three-electron reduction process is observed (−0.3 V), with two electrons being transferred to the $CBPQT^{4+}$ ring and one to the $BIPY^{2+}$ of the macrocyclic polyether. Following this three-electron transfer, the RSCC becomes the predominant translational isomer in solution on account of the radical–radical interactions that ensue between the $BIPY^{\bullet+}$ radical cations of the ring and the macrocyclic polyether. This result has been previously confirmed[22] by spectroelectrochemistry.

A one-electron process is observed at −0.77 V (peak potential), assignable to the reduction of the unpaired $BIPY^{\bullet+}$

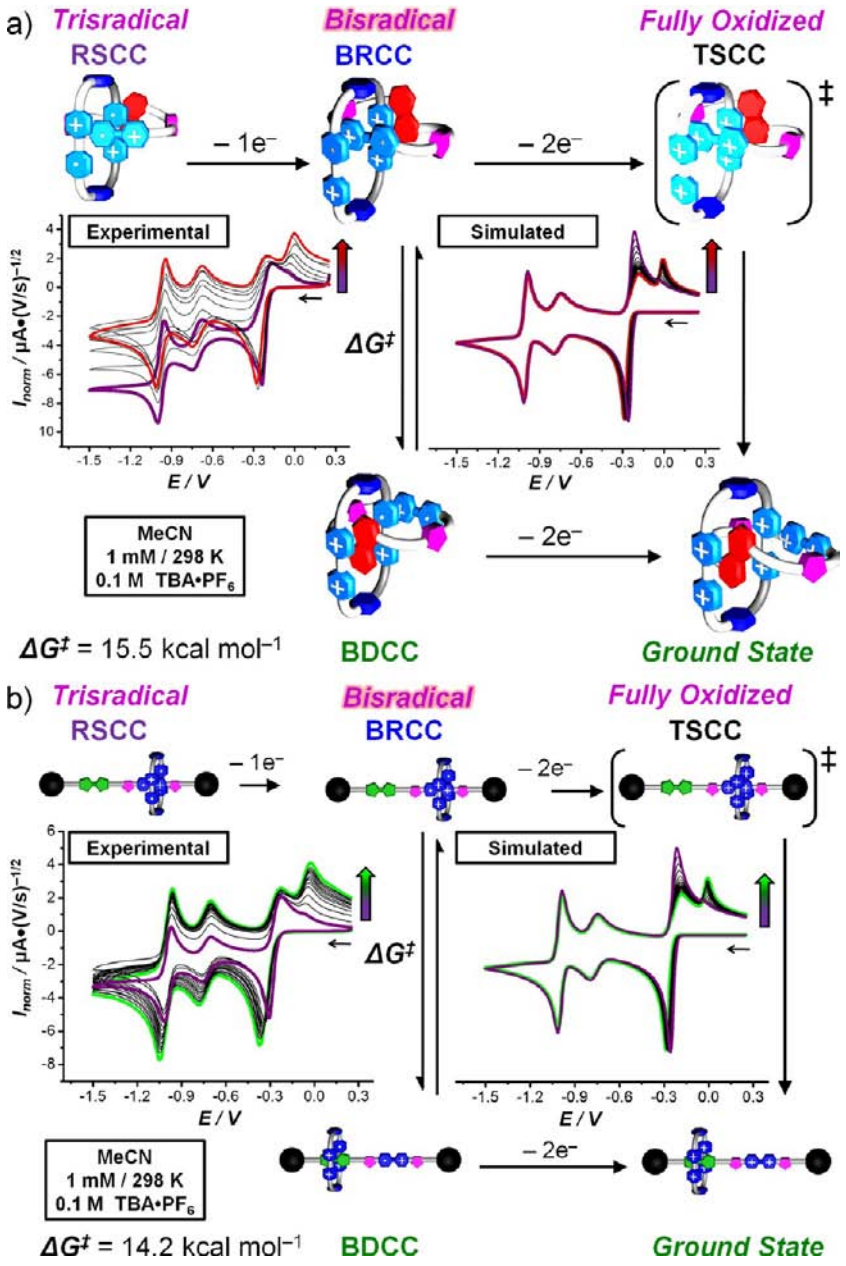

Figure 1. (a) Variable scan-rate CV of the [2]catenane $\mathbf{C1}^{6+}$, its proposed mechanism for electrochemical switching, and the digitally simulated data generated from the proposed mechanism. The purple trace was obtained at a scan rate of 20 mV s^{-1}, while intermediate traces recorded at higher scan rates are shown in black leading up to a scan rate of 1000 mV s^{-1}, shown as the red trace. The reoxidation peak at 0 V increases in relative intensity in comparison to the reoxidation peak observed at −0.25 V with faster scan rates. (b) Variable scan-rate CV of the [2]rotaxane $\mathbf{R2}^{6+}$, proposed mechanism, and digitally simulated data. The purple trace was recorded at a scan-rate of 50 mV s^{-1} with intermediate traces taken at higher scan rates shown in black, leading up to a scan rate of 1200 mV s^{-1} shown as the green trace. The reoxidation peak at 0 V increases in relative intensity with faster scan rates. Both the catenane $\mathbf{C1}^{6+}$ and $\mathbf{R2}^{6+}$ were found to display the same basic mechanism underlying their electrochemical switching processes. In particular, the observed scan-rate-dependent nature of the CV traces of both MIMs is explained by an equilibrium between two coconformations in their bisradical electronic states.

radical cation unit of the $CBPQT^{2(\bullet+)}$ ring, while a two-electron process observed at −1.10 V (peak potential) is the result of the simultaneous transfer of electrons to the remaining paired $BIPY^{\bullet+}$ radical cations. The return scan shows that these two redox processes are independent of scan rate (20−1000 mV s^{-1}) and are totally reversible.

Reoxidation of the trisradical RSCC displays, however, scan-rate-dependent behavior similar to that observed previously[17j] for a trisradical host−guest complex. On scanning at a slow rate, a single broad three-electron reoxidation peak is observed at −0.25 V. At faster and faster scan rates, it becomes apparent that reoxidation of the trisradical RSCC occurs via two different reoxidation processes. As the scan rate is increased, an oxidation peak at 0 V emerges. The oxidation process at −0.25 V is assigned to the one-electron oxidation of the unpaired $BIPY^{\bullet+}$ unit of the $CBPQT^{2(\bullet+)}$ ring, while the peak at 0 V is assigned to the simultaneous oxidation of the two spin-paired $BIPY^{\bullet+}$ units in a singlet state. In order to explain the scan-rate-dependent behavior, we have proposed a mechanism of switching involving the bisradical intermediate in which the

dx.doi.org/10.1021/ja306044r | J. Am. Chem. Soc. 2012, 134, 16275−16288

$CBPQT^{(\bullet+)(2+)}$ ring undergoes shuttling from the $BIPY^{\bullet+}$ (BRCC) to the DNP (BDCC) unit. This shuttling motion occurs[23] on account of the fact that the $CBPQT^{(\bullet+)(2+)}$ ring is capable of recognizing both radicals and π-electron-rich donors. Once encircled around the DNP unit as a consequence of donor−acceptor interactions, reoxidation of the resulting unpaired $BIPY^{\bullet+}$ radical cations shifts to more negative voltages, resulting in a single broad reoxidation peak. If insufficient time is allowed for shuttling to occur, reoxidation of the bisradical occurs as the BRCC, i.e., the two $BIPY^{\bullet+}$ radicals are still paired as they undergo oxidation. This oxidation results in formation of the TSCC for a very brief period before it relaxes back to the ground state, where the $CBPQT^{4+}$ ring encircles the DNP unit exclusively. X-Ray crystallography supports the existence of the BRCC intermediate in the solid state. Digital simulations modeled on the basis of the proposed mechanism agree well with the experimental data. Comparison with the simulated data leads to a rate of shuttling of 25 s^{-1}, a rate which corresponds to a free energy barrier to shuttling of 15.5 kcal mol^{-1} at room temperature.

[2]Rotaxanes ***R1***$^{6+}$ *and* ***R2***$^{6+}$. The syntheses of the [2]-rotaxanes $\mathbf{R1}^{6+}$ and $\mathbf{R2}^{6+}$ were achieved by following previously reported procedures.[17h] We also investigated $\mathbf{R1}^{6+}$ and $\mathbf{R2}^{6+}$ which are composed of the $CBPQT^{4+}$ ring mechanically interlocked with dumbbells containing $BIPY^{2+}$ and DNP or TTF, units, respectively, by variable scan-rate CV. Similar variable scan-rate-dependent behavior was observed (Figure 1b and SI) with these rotaxanes in comparison with the [2]catenane $\mathbf{C1}^{6+}$, an observation which indicates a similar electrochemical switching mechanism is operating within these different MIMs. For both $\mathbf{R1}^{6+}$ and $\mathbf{R2}^{6+}$, at relatively fast scan rates, a reoxidation peak is observed at 0 V. At relatively slow scan rates, this second reoxidation peak is not observed, rather only a single broad reoxidation peak. In accordance with the proposed mechanism of switching for the catenane $\mathbf{C1}^{6+}$, the bisradical forms of $\mathbf{R1}^{6+}$ and $\mathbf{R2}^{6+}$ both involve shuttling of the $CBPQT^{(\bullet+)(2+)}$ ring from the $BIPY^{\bullet+}$ unit (BRCC) to the π-electron-rich DNP or TTF units (BDCC), respectively. By comparing the experimental with the simulated data[24] based on the proposed mechanism, we have ascertained a barrier to shuttling of the $CBPQT^{(\bullet+)(2+)}$ ring from the BRCC to the BDCC to be equal to 16.1 and 14.2 kcal mol^{-1} for $\mathbf{R1}^{6+}$ and $\mathbf{R2}^{6+}$, respectively.

On comparing $\mathbf{R1}^{6+}$ with $\mathbf{R2}^{6+}$, the difference in the barrier to shuttling (Figure 2) from the BRCC to the BDCC is 1.9 kcal mol^{-1}. This difference in the barriers to shuttling is approximately equal to the difference in binding energies[11c] between the TTF-DEG ⊂ $CBPQT^{4+}$ and DNP-DEG ⊂ $CBPQT^{4+}$ (DEG = diethylene glycol) [2]pseudorotaxanes when they are measured in MeCN. We hypothesize, that the affinity of the π-donor in the dumbbell component for the dicationic $BIPY^{2+}$ unit of $CBPQT^{(\bullet+)(2+)}$ ring has a stabilizing influence on the transition state involved in the shuttling of the $CBPQT^{(\bullet+)(2+)}$ ring from the BRCC to the BDCC, a situation which we will discuss in more detail in the case of the rotaxane $\mathbf{R3}^{6+}$.

Tristable [2]Rotaxane ***R3***$^{6+}$. With the discussion of the relaxation of the bistable [2]rotaxanes $\mathbf{R1}^{6+}$ and $\mathbf{R2}^{6+}$ complete, we will now turn our attention toward a consideration of the tristable [2]rotaxane $\mathbf{R3}^{6+}$ incorporating both TTF and DNP recognition sites as well as the $BIPY^{2+}$ unit located between the two π-electron-rich donor sites. It is important to note the significance of the $BIPY^{2+}$ unit being located centrally between

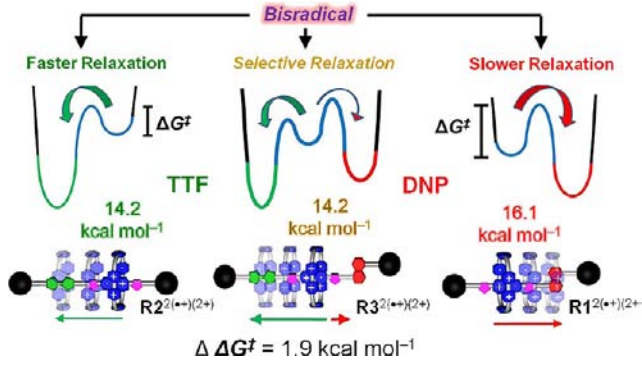

Figure 2. Thermodynamic landscapes constructed from variable scan-rate CV data of the three rotaxanes $\mathbf{R1}^{6+}$, $\mathbf{R2}^{6+}$, and $\mathbf{R3}^{6+}$ depicting the mechanical switching motion of the $CBPQT^{(\bullet+)(2+)}$ ring in the case when all three of these rotaxanes are in their bisradical tetracationic redox states. The $CBPQT^{(\bullet+)(2+)}$ ring starts out encircling the $BIPY^{\bullet+}$ unit of the dumbbell component as the BRCC. The ring then undergoes translational motion in order to encircle the π-electron-rich units (DNP or TTF) in the BDCC at a rate governed by the free energy barriers $\Delta G^{\ddagger}$ as shown. The rate of shuttling is faster in the case of $\mathbf{R2}^{6+}$ than in the case of $\mathbf{R1}^{6+}$ by over an order of magnitude. In the case of $\mathbf{R3}^{6+}$, the rate of shuttling is experimentally the same as the rate measured for $\mathbf{R2}^{6+}$, pointing strongly to the fact that shuttling of the $CBPQT^{4+}$ ring occurs in a mechanostereochemically selective fashion toward the TTF unit.

the TTF and DNP units. Similar scan-rate-dependent behavior was also observed (see SI) in the case of this rotaxane. Upon a one-electron oxidation of the trisradical RSCC of the rotaxane $\mathbf{R3}^{6+}$ to form the BRCC, *a priori*, the $CBPQT^{(\bullet+)(2+)}$ ring has two options: it can either undergo translation (i) to encircle the TTF unit or in the opposite direction (ii) to encircle the DNP unit. In the knowledge that the barrier to relaxation is significantly lower in the rotaxane $\mathbf{R2}^{6+}$ incorporating TTF compared to that of the rotaxane $\mathbf{R1}^{6+}$ incorporating DNP, we would expect the shuttling of the $CBPQT^{(\bullet+)(2+)}$ ring in the BRCC of the tristable rotaxane $\mathbf{R3}^{6+}$ to favor translation predominantly to the TTF unit, rather than to the DNP unit. The variable scan-rate behavior of $\mathbf{R3}^{6+}$ is illustrated in the SI. By simulation, the barrier to shuttling of the $CBPQT^{(\bullet+)(2+)}$ ring was measured to be 14.2 kcal mol^{-1}, a $\Delta G^{\ddagger}$ value which is experimentally the same as that determined for the rotaxane $\mathbf{R2}^{6+}$. These data suggest the shuttling (Figure 2) in the BRCC of the tristable [2]rotaxane $\mathbf{R3}^{6+}$occurs predominantly toward having the $CBPQT^{(\bullet+)(2+)}$ ring encircle the TTF unit in the BDCC. Variable-temperature, variable scan-rate CV experiments reveal (see SI) that this shuttling motion is a thermally activated mechanical process, with the rate of shuttling becoming slower with decreasing temperature. It is important to realize this fact when considering the hypothesis that the presence of the $BIPY^{2+}$ dication in the $CBPQT^{(\bullet+)(2+)}$ component may act to repel the ring from the $BIPY^{\bullet+}$ of the dumbbell as a consequence of Coulombic repulsion—a process that would not be reliant on thermal energy. This hypothesis can be discredited, however, since the rate of shuttling is indeed temperature dependent. From the variable-temperature, variable scan-rate CV experiments, we were able to determine that the enthalpic $\Delta H^{\ddagger}$ and entropic $\Delta S^{\ddagger}$ contributions to the transition-state energy for this shuttling process are +17.6 kcal mol^{-1} and +11.2 cal mol^{-1} K^{-1}, respectively. These activation parameters stand in contrast[11c] to those ($\Delta H^{\ddagger}$ = +8.4 kcal mol^{-1}, $\Delta S^{\ddagger}$ = −31 cal mol^{-1} K^{-1}) associated with the shuttling

dx.doi.org/10.1021/ja306044r | J. Am. Chem. Soc. 2012, 134, 16275−16288

of the CBPQT^{4+} ring from DNP to a bispyrrol-TTF unit obtained for a previously reported[11c] bistable [2]rotaxane employing these components. We hypothesize that the comparatively large enthalpic contribution to the barrier associated with the shuttling of the CBPQT$^{(\bullet+)(2+)}$ ring is a consequence of the energy required to unpair[25] the radical electrons of two interacting BIPY$^{\bullet+}$ radical cations before any mechanical motion can occur. We also propose that the transition state is further stabilized by folding[10h] of the flexible oligoethylene glycol chains that result when intramolecular donor–acceptor interactions[14e] occur between the BIPY^{2+} unit of the ring and the TTF unit of the dumbbell. These intramolecular donor–acceptor interactions also explain the differences in the $\Delta G^{\ddagger}$ values between **R1**$^{6+}$ and **R2**$^{6+}$ as well as between **R1**$^{6+}$and the catenane **C1**$^{6+}$. The fact that the difference in the energy barriers to shuttling for **R1**$^{6+}$ and **R2**$^{6+}$ is 1.9 kcal mol^{-1}, approximately the difference in the binding energy[11c] between the CBPQT^{4+} ring with diethylene glycol derivatives of TTF (−7.66 kcal mol^{-1}) and DNP (−6.26 kcal mol^{-1}), respectively, provides further evidence in support of the hypothesis. The greater affinity of TTF for the BIPY^{2+} unit of the CBPQT$^{(\bullet+)(2+)}$ ring results in increased stabilization of the transition state than does the DNP unit, and so the barrier to shuttling is larger in the case of the rotaxane **R1**$^{6+}$. The fact that the barrier to shuttling is slightly lower in the case of the catenane **C1**$^{6+}$ compared to **R1**$^{6+}$ is a result of the geometry of the macrocyclic polyether, which enforces[26] stabilizing donor–acceptor interactions of the DNP with the BIPY^{2+} unit. All these kinetic data for **C1**$^{6+}$, **R1**$^{6+}$, **R2**$^{6+}$, and **R3**$^{6+}$ are summarized in Table 1.

Table 1. Kinetic Parameters Associated with the Shuttling Motion of the CBPQT$^{(\bullet+)(2+)}$ Ring from the BIPY$^{\bullet+}$ Unit (BRCC) to the π-Electron-Rich Unit (BDCC) in the Bisradical Tetracationic Redox State for R1^{6+}, R2^{6+}, R3^{6+}, and C1^{6+} in 0.1 M TBA·PF$_6$ in MeCN at 298 K

	k_f s^{-1}	$\Delta G^{\ddagger}$ kcal mol^{-1}	$\Delta H^{\ddagger}$ kcal mol^{-1}	$\Delta S^{\ddagger}$ cal mol^{-1} K^{-1}
R1^{6+}	10	16.1	–	–
R2^{6+}	250	14.2	–	–
R3^{6+}	250	14.2	17.6	11.2
C1^{6+}	25	15.5	–	–

In order to provide additional evidence from CV (Figure 3), that after the one-electron reoxidation of the trisradical RSCC to the bisradical BRCC of the [2]rotaxane **R3**$^{6+}$, shuttling of the CBPQT$^{(\bullet+)(2+)}$ ring occurs predominantly in the direction of the TTF unit, we employed TTF as a redox probe[27] for the position of the ring. In a previous communication[14c] dealing with the tristable [2]rotaxane **R3**$^{6+}$, we reported on extending the lifetime of the MSCC that has the CBPQT^{4+} ring encircled around the DNP unit through incorporation of the BIPY^{2+} unit. This BIPY^{2+} unit acts as an electrostatic barrier to relaxation of the MSCC to the GSCC, which has the CBPQT^{4+} ring encircled around the TTF unit. Upon oxidation of the TTF unit, the CBPQT^{4+} ring is very quickly repelled along a pathway activated by Coulombic energy over the BIPY^{2+} electrostatic barrier to encircle the DNP unit. Upon reduction of the TTF^{2+} dication back to its neutral state, the CBPQT^{4+} ring remains around the DNP unit for some time before passing over the BIPY^{2+} barrier by means of a thermally activated process accessing the TSCC as the transition state to this shuttling in

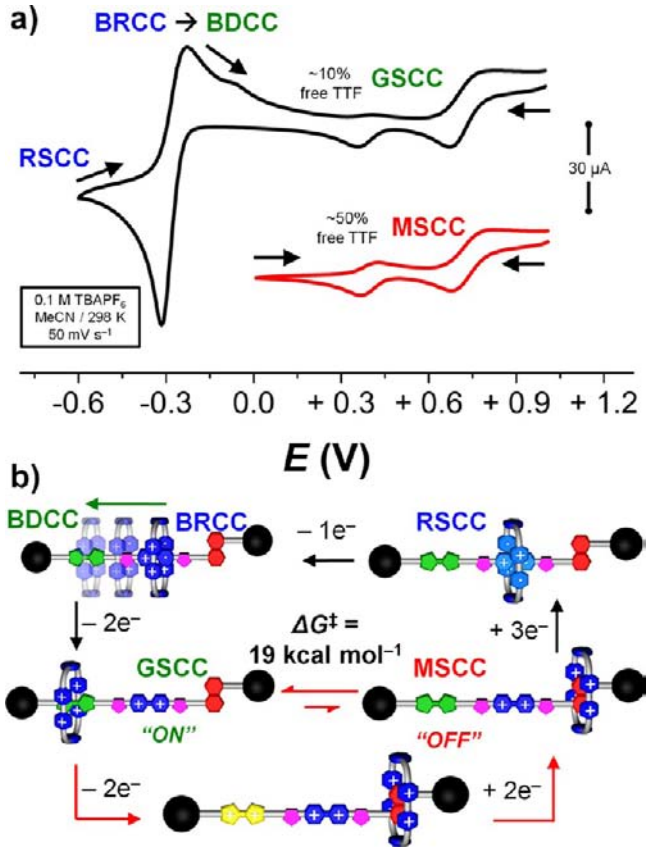

Figure 3. (a) The red trace CV taken at a scan rate of 50 mV s^{-1} of the [2]rotaxane **R3**$^{6+}$ reveals evidence for the formation of the MSCC through an oxidation–reduction cycle of the TTF moiety. The CV begins at +1 V, with the oxidation of the TTF unit to its TTF^{2+} dication, which repels the tetracationic CBPQT^{4+} ring over the BIPY^{2+} electrostatic barrier to encircle the DNP unit. Scanning toward 0 V reduces the TTF^{2+} dication back to its neutral form, resulting in the MSCC wherein the CBPQT^{4+} remains encircled for some time around the DNP subunit before passing over the BIPY^{2+} electrostatic barrier back onto TTF to form the GSCC. At this scan rate, the amount of "free" TTF still remaining, as measured from the return scan, is 50%. The black trace CV also recorded at a scan rate of 50 mV s^{-1} starting at +1 V, but with the scan limit of −0.60 V, which is enough to ensure the formation of the RSCC. The return scan shows that the amount of free TTF is now only 10% and corresponds to the GSCC/MSCC distribution ratio of 10:1 at equilibrium. (b) Schematic representation for the formation of the MSCC which can be reset to the GSCC through thermal relaxation or by accessing the RSCC in the pathway described above.

order to encircle the TTF unit once again, restoring the ground-state distribution of 10:1/GSCC:MSCC. This relaxation is governed[14c] by a barrier of 19 kcal mol^{-1} in MeCN at 298 K with 0.1 M TBA·PF$_6$, an increase of 3 kcal mol^{-1} from the previously reported[11c] [2]rotaxane, omitting the central BIPY^{2+} moiety.

In the CV, we scanned (Figure 3a) at 50 mV s^{-1} a potential window, starting at +1 V and reversing the scan at −0.60 V. Starting at +1 V generates the TTF^{2+} dication, enticing the CBPQT^{4+} ring to pass over the BIPY^{2+} electrostatic barrier and encircle the DNP unit. Rereduction of TTF^{2+} dication occurs by means of two one-electron processes, after which the CBPQT^{4+} ring remains encircled around the DNP unit, kinetically trapped before passing over the electrostatic BIPY^{2+} barrier to encircle the more favored TTF unit. Scanning

dx.doi.org/10.1021/ja306044r | J. Am. Chem. Soc. 2012, 134, 16275–16288

further past 0 V toward −0.60 V invokes the three-electron reduction process, generating the RSCC. It is important to note that prior to this three-electron reduction, the $CBPQT^{4+}$ ring has not had enough time to relax fully back to the TTF unit, a conclusion which can be reached by taking a scan only to the potential of 0 V and back. In this CV experiment, approximately 50% of free TTF still exists, which is significantly far from the equilibrium distribution of 10% free TTF, i.e., 10:1/GSCC:MSCC. A scan rate of 50 mVs^{-1} is slow enough such that (i) nearly all of the BRCC generated after the initial one-electron oxidation is allowed to shuttle to the BDCC and (ii) becomes reoxidized after shuttling has occurred, as indicated by the observation that almost no second reoxidation peak at 0 V can be detected. Scanning further past 0 V toward +1 V reveals two oxidation peaks, the first of which corresponds to the initial oxidation of free TTF, followed by the oxidation of encircled TTF combined with the second oxidation of free TTF. Quantification of the relative amount of free TTF from an integration analysis of these two oxidation peaks reveals that the amount of free TTF detected, after proceeding through a reoxidation pathway where only the BDCC is oxidized (and not the BRCC), is approximately 10%, a percentage that is consistent with the ground-state equilibrium distribution ratio. These results provide strong evidence that, after the one-electron oxidation of the trisradical RSCC of the tristable rotaxane $\mathbf{R3}^{6+}$ to form the BRCC, the $CBPQT^{(\bullet+)(2+)}$ of the BRCC shuttles in a *mechanostereochemical selective* fashion onto TTF in the BDCC (Figure 3b) as a consequence of the faster kinetics associated with this process in comparison with translation toward the DNP unit. Furthermore, by taking advantage of this mechanostereochemical selective pathway forged out by the trisradical species, we can restore the rotaxane to its GSCC.

Since it is possible to control the reoxidation pathway depending on the scan rate employed, we investigated further how the $CBPQT^{4+}$ ring is propelled when the reoxidation occurs, while in the BRCC, wherein $CBPQT^{(\bullet+)(2+)}$ is still encircling the $BIPY^{\bullet+}$ radical cation, forming the TSCC. We performed a similar experiment (Figure 4a) by scanning a potential window starting at +1 V and reversing the scan at −0.60 V, only this time, at 1000 mV s^{-1}. This scan rate is fast enough to ensure that almost none of the BRCC has had time to shuttle to the BDCC, and so nearly all the oxidation will occur while the ring is encircled around the $BIPY^{\bullet+}$ radical cation corresponding to the TSCC for the rotaxane $\mathbf{R3}^{6+}$. Starting at a potential of +1 V generates the TTF^{2+} dication. Scanning toward 0 V reduces the TTF^{2+} back to its neutral state through two one-electron processes. Scanning further toward −0.60 V forms the trisradical RSCC. In this reoxidation pathway, the highly transient TSCC is momentarily attained as a result of the second two-electron oxidation at 0 V, that follows after the first one-electron oxidation of the non-interacting $BIPY^{\bullet+}$ of the $CBPQT^{2(\bullet+)}$ ring encircling the $BIPY^{\bullet+}$ of the dumbbell component. The TSCC is not stable since it possesses a large amount of Coulombic potential energy, and *a priori*, the $CBPQT^{4+}$ ring has two choices once again − it can either be repelled toward the TTF unit or toward the DNP unit. Scanning past 0 V toward +1 V reveals two one-electron oxidation processes corresponding to the first oxidation of free TTF and a combination of the first oxidation of encircled TTF and the second oxidation of free TTF. Quantification of these oxidation waves reveals the existence of approximately 30% free TTF, indicating that a majority of the ring has been pushed onto the TTF unit rather than onto the DNP unit from the TSCC. It is important to note that, prior to reduction, approximately 90% of the $CBPQT^{4+}$ ring is still located on the DNP unit. The amount of free TTF can be reduced by 60 to 30% on going along this reoxidation pathway, relying only upon the TSCC, which is almost the GSCC equilibrium of 10% free TTF. Taken together, these results demonstrate (Figure 4b) that the restoration of the GSCC can be achieved through a redox-activated pathway, and the reliance on an entirely thermally activated pathway is not necessary.

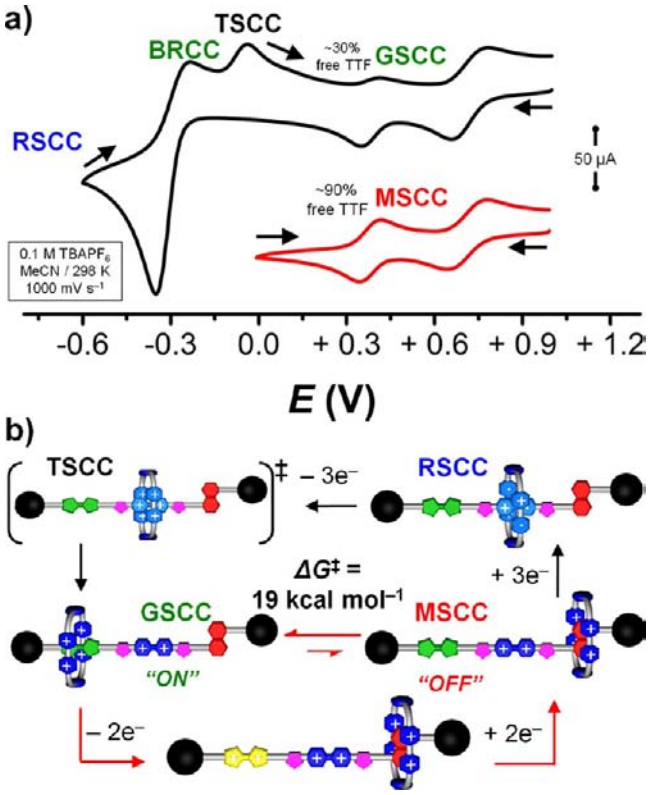

Figure 4. (a) The red trace CV recorded at a scan rate of 1000 mV s^{-1} of the [2]rotaxane $\mathbf{R3}^{6+}$ provides evidence for the formation of the MSCC as a result of an oxidation−reduction cycle implemented on the TTF unit. The CV begins at +1 V with the oxidation of the TTF unit to its TTF^{2+} dication, which repels the tetracationic $CBPQT^{4+}$ ring over the $BIPY^{2+}$ electrostatic barrier to encircle the DNP unit. Scanning toward 0 V reduces the TTF^{2+} dication back to its neutral state, forming the MSCC, wherein the $CBPQT^{4+}$ ring remains encircled for some time around the DNP unit before passing over the $BIPY^{2+}$ electrostatic barrier back onto the TTF unit to form the GSCC. At this scan rate, the amount of "free" TTF still remaining, as measured by the return scan, is 90%. The black trace CV also taken at a scan rate of 1000 mV s^{-1} also starts at +1 V but with the scan limit of −0.60 V, which is enough to ensure the formation of the RSCC. The return scan shows that the amount of free TTF is now only 30%. (b) Schematic representation for the formation of the MSCC, which can be reset to the GSCC through thermal relaxation or by going through the RSCC in the pathway discussed above.

X-Ray Crystallography. The solid-state structure of the fully oxidized $\mathbf{C1}\cdot 6PF_6$ was previously reported[22] by us, and we have reproduced a depiction of it here for the sake of convenience. In particular, the structure reveals (Figure 5a) that the DNP unit is located inside the cavity of the $CBPQT^{4+}$ ring, while the $BIPY^{2+}$ unit is located as far as possible as a result of Coulombic repulsion. We now report our investigation of the catenane in its reduced form. Solid-state evidence of the

dx.doi.org/10.1021/ja306044r | J. Am. Chem. Soc. 2012, 134, 16275−16288

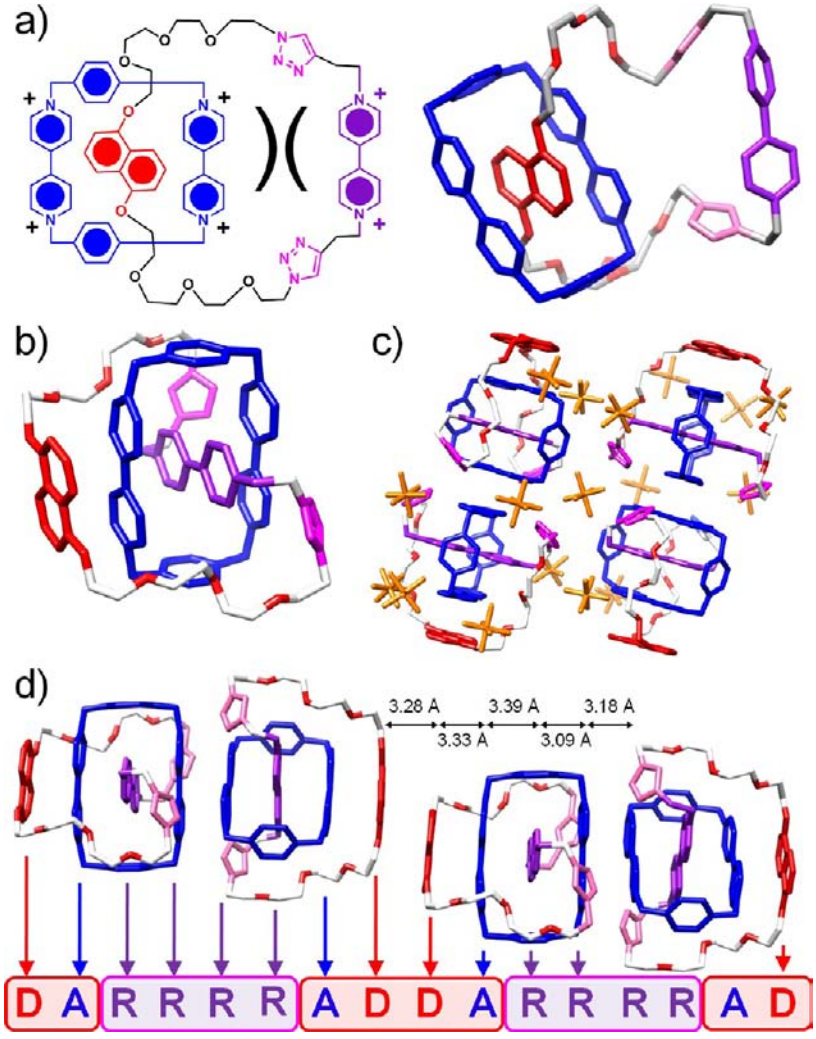

Figure 5. (a) Structural formula and solid-state structure of $\mathbf{C1}^{6+}$ in its fully oxidized hexcationic redox state. In this redox-state, donor−acceptor interactions result in inclusion of the DNP unit inside the cavity of the $CBPQT^{4+}$ component, while Coulombic repulsion forces the $BIPY^{2+}$ of the macrocyclic polyether far away. (b) Solid-state structure obtained from single crystal X-ray analysis of the catenane $\mathbf{C1}^{2(\bullet+)(2+)}$ in its bisradical tetracationic redox state. The bisradical catenane $\mathbf{C1}^{2(\bullet+)(2+)}$ is observed to exist as the BRCC translational isomer, in which the $BIPY^{\bullet+}$ unit of the macrocyclic polyether is encircled by the $CBPQT^{(\bullet+)(2+)}$ ring. The ratio of PF_6^- counterions to catenane molecules was determined to be 4:1, an observation which provides evidence for the bisradical tetracationic redox state. The PF_6^- counterions are omitted for the sake of clarity. (c) The unit of cell of the single crystal of $\mathbf{C1}^{2(\bullet+)(2+)}$ containing four catenane molecules all positioned around a center of inversion. (d) The extended solid-state superstructure of the catenane $\mathbf{C1}^{2(\bullet+)(2+)}$ showing a continuous stack of discrete domains of radical−radical and donor−acceptor interactions between $BIPY^{\bullet+}$ radical cation and $BIPY^{2+}$/DNP units, respectively.

bisradical redox state has been obtained by single crystal X-ray crystallography. The [2]catenane $\mathbf{C1}\cdot 6PF_6$ was dissolved in MeCN, and excess of zinc dust[17j] was added to the solution in order to reduce the catenane to its trisradical form. Slow vapor diffusion of $i Pr_2O$ into this solution after removal of the zinc dust afforded single crystals suitable for X-ray analysis. The solid-state structure[28] reveals (Figure 5b,c) that there are four PF_6^- counterions per catenane molecule, an observation which implies the catenane is in the bisradical tetracationic $\mathbf{C1}^{2(\bullet+)(2+)}$ state, even though the initial solution comprised[22] the catenane in its trisradical form. The $BIPY^{\bullet+}$ radical cation component of the macrocyclic polyether resides inside the cavity of the $CBPQT^{(\bullet+)(2+)}$ ring, while the DNP unit is located alongside. The $BIPY^{\bullet+}$ radical cation is located inside the cavity at an angle of 13° from the principal axis of the cyclophane. We hypothesize[29] that this relative orientation maximizes the amount of π-orbital overlap with the $BIPY^{\bullet+}$ radical cation of the ring. The unit cell of the crystal contains four catenane molecules located around a center of inversion. Analysis of the plane-to-plane separation between the $BIPY^{\bullet+/2+}$ and DNP units provides further evidence that the [2]catenane is present in its bisradical form, allowing us to make definitive assignments to the dicationic $BIPY^{2+}$ and radical cationic $BIPY^{\bullet+}$ units. The $BIPY^{\bullet+}$ radical cation unit inside the cavity of the $CBPQT^{(\bullet+)(2+)}$ ring is located closer to one side of the ring than the other. The plane-to-plane separation of the outside $BIPY^{\bullet+}$ radical cation of the ring with the $BIPY^{\bullet+}$ radical cation of the macrocyclic polyether is 3.09 Å, while the plane-to-plane separation with respect to the $BIPY^{2+}$ dication is 3.39 Å. The plane-to-plane distance between the DNP unit and the dicationic $BIPY^{2+}$ unit is 3.33 Å, a distance which is consistent with π-stacking[30] brought about by donor−acceptor π-orbital overlap. Furthermore, the torsional twists of all $BIPY^{\bullet+}$ and $BIPY^{2+}$ units about their 4,4′-C−C bonds are less than 6°. It is known[17j,31] that this relatively small twist is observed in the case when $BIPY^{\bullet+}$ units have been reduced to their radical cationic

dx.doi.org/10.1021/ja306044r | J. Am. Chem. Soc. 2012, 134, 16275−16288

forms or when $BIPY^{2+}$ dications are engaged[9e,10a] in donor–acceptor interactions, in comparison to free $BIPY^{2+}$. This effect, which produces a reduction in the torsional angles of the $BIPY^{2+/\bullet+}$ units, is a direct result of electron density populating π-antibonding orbitals, which leads to increased double-bond character between the 4,4′-C–C bonds. As a result, this bond is also observed to decrease in length compared with the bond in free $BIPY^{2+}$ dications, while the $3^{(\prime)}$,$4^{(\prime)}$/$4^{(\prime)}$,$5^{(\prime)}$-C–C bond lengths are all observed to increase. In the case of reduced $BIPY^{\bullet+}$ radical cations, an entire electron is populating the antibonding orbital, so these bond distortions are even more exaggerated compared to the case of the $BIPY^{2+}$ units engaged in donor–acceptor interactions, where only partial electron density is populating this orbital. Nonetheless, the end result is the same (Table 2) for both donor–acceptor and radical–

Table 2. Bond Length and Torsional Data Obtained from Crystallographic Analysis of $BIPY^{2+}$ and $BIPY^{2+}$-DNP Dications and $BIPY^{\bullet+}$ Radical Cations[a]

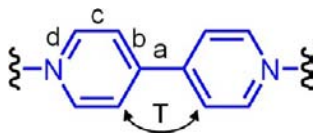

	a, Å	*b*, Å	*c*, Å	*d*, Å	*T*, °
$BIPY^{2+}(CBPQT^{4+})$[b]	1.48	1.39	1.38	1.34	40.0
$BIPY^{2+}$-DNP $(C^{2(\bullet+)(2+)})$[c]	1.48	1.40	1.37	1.34	3.5
$BIPY^{\bullet+}(C^{2(\bullet+)(2+)})$[c]	1.43	1.42	1.36	1.36	3.6

[a]Inset defines the various bond distances and torsional angle. All distances and angles correspond to an average value measured across the unit cell. [b]Data obtained from crystal data in ref 9e of the CBPQT•$4PF_6$ ring. [c]Data obtained from crystal data reported here on the [2]catenane $C^{2(\bullet+)(2+)}$•$4PF_6$.

radical interactions pointing to the similarities[32] in the fundamental orbital interactions between these two seemingly different recognition motifs.

The solid-state extended packing structure (Figure 5d) is also consistent with the bisradical state and provides insight as to why the bisradical state of the catenane is the one which is isolated in solution, even though the initial solution contained the trisradical form of the catenane. The outside $BIPY^{\bullet+}$ radical cation of the $CBPQT^{(\bullet+)(2+)}$ ring π-stacks with another outside $BIPY^{\bullet+}$ radical cation from an adjacent catenane molecule, with a plane-to-plane separation of 3.18 Å. In a similar fashion, the DNP unit is observed to be π-stacked, although in an offset fashion, with another DNP unit from an adjacent catenane molecule on the opposite side, with a plane-to-plane separation of 3.28 Å. This interplanar π–π stacking motif between two $BIPY^{\bullet+}$ radical cations on one side and two DNP units on the other continues throughout the crystal in such a manner as to form one continuous stack replete with discrete domains of radical–radical and donor–acceptor interactions. We believe that this stacking arrangement brings about an element of stability which is not possible to achieve if the catenane were in its trisradical form. When in the trisradical form, the DNP unit is not able to enter into donor–acceptor interactions with the inside $BIPY^{\bullet+}$ radical cation of the ring and will find itself as a "fifth wheel", disrupting the favorable extended packing structure. Overall, the observation of the bisradical in the solid-state crystal structure supports the mechanism of switching in solution, which sees the bisradical as an intermediate state as one where the $CBPQT^{(\bullet+)(2+)}$ ring can be engaged in either donor–acceptor or radical–radical interactions.

UV–vis Spectroscopy. In order to confirm the results obtained from CV, namely, the fact that the MSCC can be restored to the GSCC through accessing the RSCC, UV–vis spectroscopic experiments were performed on the tristable rotaxane **R3**$^{6+}$ in MeCN at 263 K. The initial spectrum reveals (Figure 6a) an intense charge-transfer (CT) band centered on 840 nm, which is characteristic[27,33] of the encirclement of the $CBPQT^{4+}$ ring around a TTF unit. This observation confirms that the ground-state distribution favors the GSCC as the major translational isomer. Aliquots of an $Fe(ClO_4)_3$ solution were added in sequence in order to oxidize[27] the TTF unit of **R3**$^{6+}$. The spectra first of all shows a decrease in the intensity of the 840 nm band with the simultaneous growth of the bands centered on 440 and 600 nm, which are characteristic[27] of the $TTF^{\bullet+}$ radical cation. When further aliquots of $Fe(ClO_4)_3$ solution were added, the 440 and 600 nm bands disappeared, and a new band, which is characteristic[27] of the TTF^{2+} dication, resulted at 363 nm. Furthermore, a low-intensity CT band centered on 530 nm indicates[9e] the encirclement of the $CBPQT^{4+}$ ring around the DNP unit.

In order to reduce the TTF^{2+} dication back to its neutral form, small quantities of zinc dust were added to the solution sequentially, while monitoring the UV–vis spectrum. The reappearance (Figure 6b) of the $TTF^{\bullet+}$ radical cation bands, followed by their subsequent decrease in intensity (Figure 6c), confirms that the TTF^{2+} dication is reduced back to its neutral form, passing through the $TTF^{\bullet+}$ radical cation as an intermediate on the way. Importantly, no CT band centered on 840 nm could be observed after the neutral TTF unit had been restored; an observation which indicates that the MSCC has been populated and trapped by the $BIPY^{2+}$ electrostatic barrier. At this point, an excess of zinc dust was added to the solution (Figure 6d) in order to reduce[17j] the $BIPY^{2+}$ units to their radical cation forms and bring about formation of the RSCC, which was evidenced by the appearance[17h,j] of intense bands centered on 541 and 860 nm. Reoxidation, by exposing the solution to ambient O_2, resulted in a drastic increase of the CT band at 840 nm, indicating that the GSCC has been restored to approximately its ground-state distribution at equilibrium. These results agree well with those obtained from CV experiments which also reveal that the MSCC can be reset to the GSCC through accessing the RSCC.

^{1}H NMR Spectroscopy. In order to lend further support to the fact that the MSCC of **R3**$^{6+}$ can be trapped by means of electrostatic repulsion and then reset back to the GSCC by accessing the RSCC, we performed ^{1}H NMR spectroscopy in CD_3COCD_3 at 233 K. The initial spectrum of **R3**·$6PF_6$ shows (Figure 7), in particular, six resonances between 7.2 and 7.6 ppm, which can be assigned[34] to the aromatic protons of the DNP. These downfield resonances associated with the DNP protons indicate that this unit is free from being encircled by the $CBPQT^{4+}$ ring, an observation which is consistent with the GSCC being the major translational isomer at equilibrium. Resonances associated with the *cis* and *trans* olefinic protons of the TTF unit encircled by the $CBPQT^{4+}$ ring were observed clustered around 6.4 ppm. Upon addition of excess oxidizing agent, tris(*p*-bromophenyl)ammoniumyl hexachloroantimonate, resonances associated with the olefinic TTF protons vanished altogether,[35] and two new resonances between 9.8 and 10.0 ppm were observed. These two resonances are associated

dx.doi.org/10.1021/ja306044r | J. Am. Chem. Soc. 2012, 134, 16275–16288

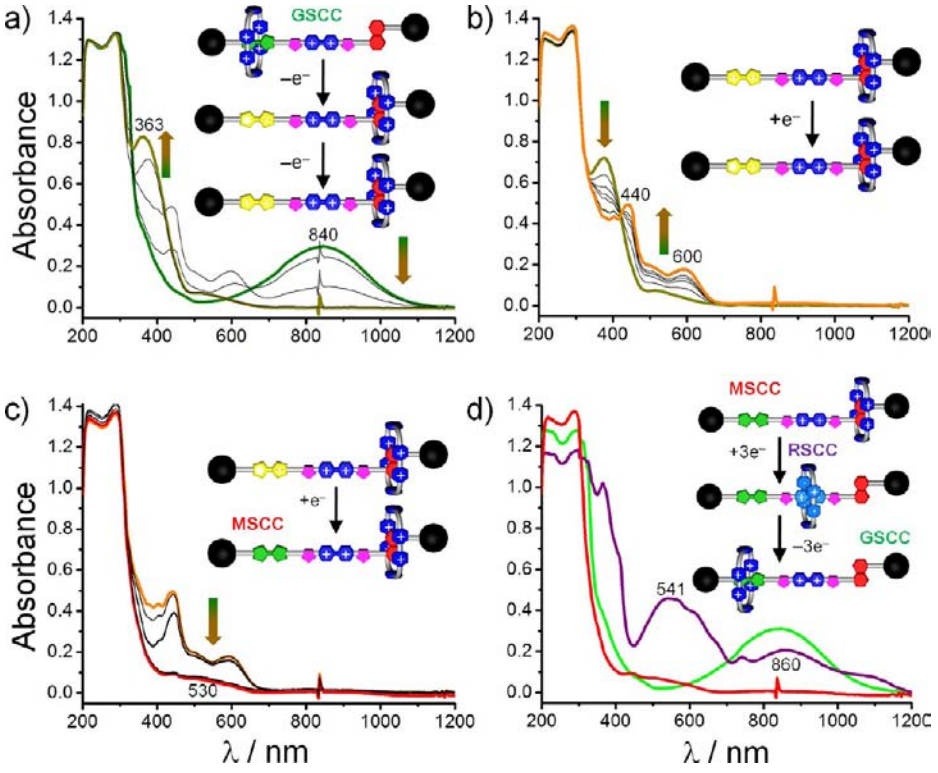

Figure 6. UV−vis spectroscopic investigation of the redox-active switching behavior of the tristable rotaxane **R3**$^{6+}$ in MeCN at 263 K. (a) Spectra obtained during the titration of a solution (10 mM) of $Fe(ClO_4)_3$ into a solution (0.1 mM) of **R3**$^{6+}$, providing evidence for the oxidation of TTF, first to its $TTF^{\bullet+}$ radical cation and then to its TTF^{2+} dication. (b) Spectra recorded after incremental additions of zinc dust to the solution of the rotaxane containing the TTF^{2+} dication, showing its reduction to the $TTF^{\bullet+}$ radical cation. (c) Further additions of zinc dust resulting in reduction of the $TTF^{\bullet+}$ radical cation to its neutral form. Note the small band at 530 nm and the lack of any strong absorption in the 840 nm region. (d) Spectra obtained after the addition of excess of zinc dust (purple trace) and following exposure to O_2 (green trace). Note the return of the strong absorption band observed at 840 nm.

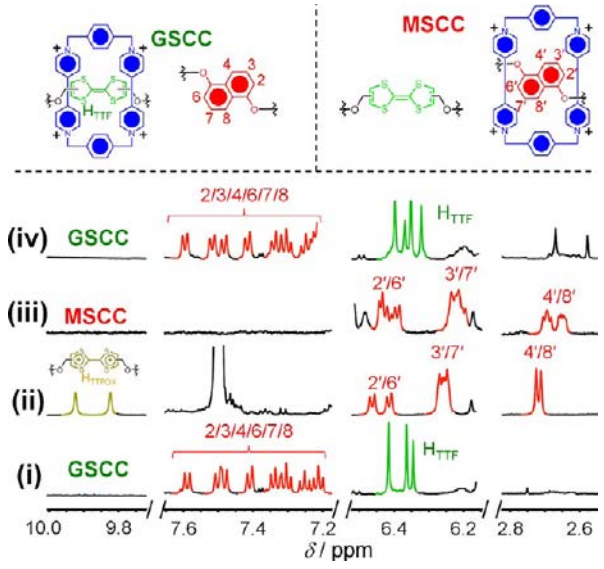

Figure 7. ^{1}H NMR spectroscopic investigation of the redox-active switching behavior of the rotaxane **R3**$^{6+}$ in CD_3COCD_3 at 233 K. (i) Partial ^{1}H NMR spectrum of the initial solution of **R3**$^{6+}$. (ii) Partial ^{1}H NMR spectrum after the addition of an excess of magic blue, revealing the oxidation of the TTF unit to its dicationic form. (iii) Partial ^{1}H NMR spectrum of the MSCC of the rotaxane **R3**$^{6+}$. (iv) Partial ^{1}H NMR spectrum of the rotaxane **R3**$^{6+}$ after treating the solution of the MSCC with an excess of zinc dust and then exposing it to O_2.

with the aromatic protons of the dicationic TTF^{2+} unit that result after oxidation. In addition, resonances located between 7.2 and 7.6 ppm, associated with the aromatic DNP protons free of the $CBPQT^{4+}$ ring, were no longer observed, and instead, a new set of peaks associated[34] with the protons of the DNP unit encircled by the $CBPQT^{4+}$ ring was observed. In particular, a new doublet which appears around 2.7 ppm that can be assigned to the 4/8 protons of the DNP unit: the doublet is shifted upfield drastically as a consequence of [C−H···π] interactions occurring[34] with the bridging *para*phenylene units present in the $CBPQT^{4+}$ ring. The resonances for the 2/6 and 3/7 DNP protons are also observed in further upfield positions between 6.2 and 6.6 ppm. The assignments of these resonances were confirmed (see the SI) by ^{1}H−^{1}H COSY spectroscopy. These results support the notion that the $CBPQT^{4+}$ ring can be made to translate over the central $BIPY^{2+}$ electrostatic barrier and onto DNP as a consequence of Coulombic repulsion associated with the TTF^{2+} dication.

Next, we prepared a pure solution of the MSCC of **R3**$^{6+}$ in CD_3COCD_3 at 233 K. Briefly, **R3**·6PF_6 was dissolved in Me_2CO, and a slight excess of $Fe(ClO_4)_3$ was added to the solution in order to oxidize the TTF unit to its dicationic form. The solution was then cooled in a dry ice acetone bath followed by the addition of an excess of ascorbic acid as a solid to serve as a reducing agent for the TTF^{2+} dication. As soon as the color of the solution became red, a saturated solution of cold aqueous NH_4PF_6 was added, and the resulting reddish purple precipitate was collected by filtration and washed with cold H_2O. The dried solid was placed in an NMR tube, dissolved in

dx.doi.org/10.1021/ja306044r | J. Am. Chem. Soc. 2012, 134, 16275−16288

CD_3COCD_3, and cooled in a dry ice acetone bath, following which the ^1H NMR spectrum was recorded at 233 K. Importantly, the spectrum reveals that the resonances associated with the protons of the TTF^{2+} dication between 9.8 and 10.0 ppm are no longer present in the spectrum, while the resonances for the aromatic DNP protons are still shifted upfield, an observation which indicates[34] that the $CBPQT^{4+}$ ring remains encircled around the DNP unit even when the TTF unit becomes neutral once again. The additional fact that the resonances for the DNP protons do not appear as perfect doublets and triplets provides further evidence that the TTF unit has been reduced to its neutral form wherein its *cis* and *trans* isomers are in slow exchange, resulting in an added degree of complexity in the observed spectrum. The kinetic stability of the MSCC is such that at these temperatures, recording a $^1H-^1H$ COSY 2D spectrum (see SI) over the course of an hour is possible. As a consequence, all the proton assignments could be corroborated by this 2D technique. If the CD_3COCD_3 solution is allowed to stand at room temperature, relaxation of the MSCC to ground-state distribution occurs (see SI) by a thermally activated pathway but only on the order[21] of days.

Zinc dust was added to the cooled solution of the MSCC of the [2]rotaxane **R3**·$6PF_6$ in order to reduce the $BIPY^{2+}$ units to their radical cations, yielding[17j] the RSCC. The solution became dark purple after a few minutes, an observation which is indicative of the formation of the trisradical state. The zinc dust was then filtered off, and while on a dry ice acetone bath, air was bubbled through the solution to introduce oxygen in order to oxidize the $BIPY^{\bullet+}$ radical cations back to their dicationic forms. After a few minutes, the purple color retreated, and a green colored solution emerged. The ^1H NMR spectrum of this green solution confirmed that the rotaxane had indeed returned to the GSCC. The resonances associated with the aromatic protons of the DNP unit once again appeared downfield between 7.2 and 7.6 ppm, indicating[34] that the DNP unit is free of the $CBPQT^{4+}$ ring. Overall, the ^1H NMR spectrum is nearly identical (see SI) to the original spectrum of the rotaxane recorded as the GSCC, prior to any redox experimentation. These results are consistent with UV−vis spectroscopic and CV experiments which show that the GSCC can be recovered from the MSCC by reduction to the RSCC, followed by reoxidation.

Quantum Mechanical Calculations. In order to examine the hypothesis that the monoradical tricationic $CBPQT^{(\bullet+)(2+)}$ ring is capable of recognizing both π-electron-rich donor molecules and radical cationic $BIPY^{\bullet+}$ units, we carried out a series of ab inito calculations on the bisradical tetracationic $CBPQT^{(\bullet+)(2+)} \subset MV^{\bullet+}$ inclusion complex using several DFT methods, including B3LYP and M06. These methods suffer, however, from self-interaction errors and do not give the correct charge distribution for this complex. Although the functionals of such DFT methods are adjusted to produce accurate energies, the actual charge distributions may not be reliable. Indeed, for these systems, the DFT charges lead to descriptions incompatible with both experiment and ab initio calculations. Therefore, we applied second-order Møller−Plesset perturbation theory (MP2) at 6-31G level to optimize the geometry in the polarizable continuum model (PCM) for acetonitrile (ε = 37.5 and R_0 = 2.18 Å).

The Löwdin charge distribution (Figure 8a) on the three $BIPY^{2+/\bullet+}$ units of the $CBPQT^{(\bullet+)(2+)} \subset MV^{\bullet+}$ complex are 1.9, 1.0, and 1.0, corresponding to the experimental charge assignment. The interplanar distance between the two $BIPY^{\bullet+}$ units is 3.04 Å, which is much shorter than the interplanar distance (3.61 Å) between the middle $BIPY^{\bullet+}$ and the $BIPY^{2+}$, indicating the favored interaction between the $BIPY^{\bullet+}$ units. The magnitude of the dihedral angle between the two pyridine units of each $BIPY^{2+/\bullet+}$ units differs according to the charge on each of these units; the dihedral angles are 26.7° for the $BIPY^{2+}$, 5.7° for the middle $BIPY^{\bullet+}$, and 0.9° for the remaining $BIPY^{\bullet+}$.

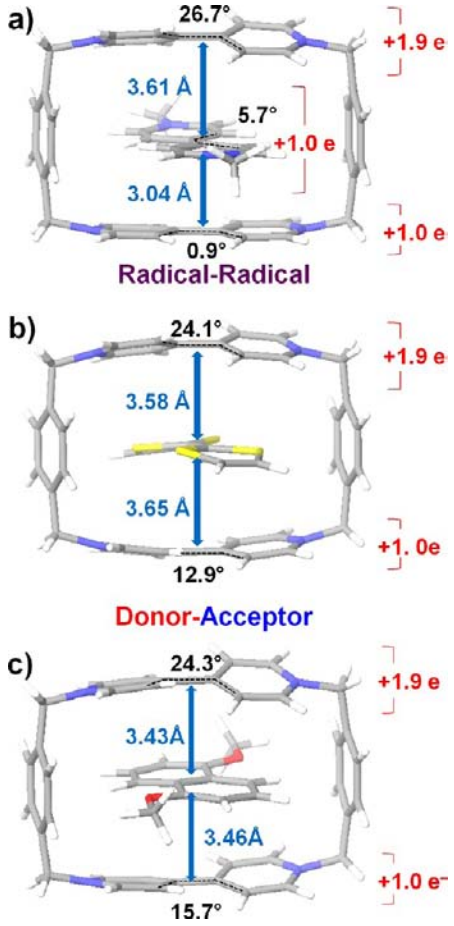

Figure 8. (a) Geometry of $CBPQT^{(\bullet+)(2+)} \subset MV^{\bullet+}$. The distance between units carrying +1e is much shorter. (b) The geometry of $CBPQT^{(\bullet+)(2+)} \subset$ TTF. (c) The geometry of $CBPQT^{(\bullet+)(2+)} \subset$ DNP. In each case, the dihedral angles between pyridines are in black, interplanar distances in blue, and the charges associated with each unit are in red. All geometries were optimized at MP2/6-31G in PCM MeCN solvent.

In the case of the inclusion complex of $CBPQT^{(\bullet+)(2+)} \subset$ TTF, the Löwdin charge distribution (Figure 8b) on the two $BIPY^{2+/\bullet+}$ units is 1.9 and 1.0. At the optimized geometry, TTF is closer to the $BIPY^{2+}$ unit. The interplanar distance to $BIPY^{\bullet+}$ is 3.65 Å, whereas it is 3.58 Å to $BIPY^{2+}$. Similar structural parameters are also found in the case of the inclusion complex of $CBPQT^{(\bullet+)(2+)} \subset$ DNP, where the Löwdin charge distributions (Figure 8c) on the two $BIPY^{2+/\bullet+}$ units are 1.9 and 1.0. At the optimized geometry, the interplanar distance from DNP to $BIPY^{\bullet+}$ is 3.46 Å, whereas to $BIPY^{2+}$, it is 3.43 Å. Without radical−radical interactions, closed-shell molecular entities, such as DNP and TTF, slightly favor $BIPY^{2+}$ unit over $BIPY^{\bullet+}$, most likely in part at least as a consequence of the stronger Coulombic interactions that polarize the π-electrons on DNP or TTF in addition to a lesser amount of Pauli-repulsion energy. These theoretical results are consistent with

dx.doi.org/10.1021/ja306044r | J. Am. Chem. Soc. 2012, 134, 16275−16288

the experimental data and confirm that the CBPQT$^{(\bullet+)(2+)}$ ring has a "split personality", behaving as both a donor- and radical-loving species at the same time.

In order to understand the delocalized spin-pairing interaction, we built a model system containing only two MV$^{\bullet+}$ units and examined the singlet−triplet (S−T) gap, an indicator of noncovalent bond strength just as in the case of covalent bonding between atoms. Calculations at the level of CASSCF(2e,2o)/cc-pVDZ plus a diffuse function show that, at the distance observed (3.15 Å) in the crystal structure, the S−T energy gap is 10.5 kcal mol^{-1} which decreases to zero as the plane-to-plane distance increases. The exponential decay of the S−T gap means that the bonding strength is proportional to the overlap of the singly occupied orbitals which decays exponentially in space. The spin pairing of the bisradical CBPQT$^{(\bullet+)(2+)}$ ⊂ MV$^{\bullet+}$ complex was investigated at the CASSCF(2e,3o)/6-31G level with PCM. One more orbital was included in the active space for the correlation from the empty orbital on BIPY^{2+} unit. We found that the bisradical intermediate CBPQT$^{(\bullet+)(2+)}$ ⊂ MV$^{\bullet+}$ is thermodynamically metastable at 5.8 kcal mol^{-1} higher (Figure 9) than the infinitely separated CBPQT$^{(\bullet+)(2+)}$ and MV$^{\bullet+}$. It is necessary, however, to break the radical bonding between two BIPY$^{\bullet+}$ units before the disassociation process occurs, making it kinetically stable. A pull-out scan of the potential energy singlet surface points to a 7.6 kcal mol^{-1} barrier height at a pull-out distance 1.6 Å. Beyond this point, the electrostatic repulsion dominates and pushes the center MV$^{\bullet+}$ out of the cavity of the ring. The 1.3 kcal mol^{-1} S−T gap at 1.6 Å suggests that this repulsion plays a role to lower the barrier, enabling the disassociation process to occur without totally breaking the noncovalent bonding between the two BIPY$^{\bullet+}$ units. This calculated barrier height of 7.6 kcal mol^{-1} is somewhat lower than the experimental value[17j] of approximately 16 kcal mol^{-1}, an outcome which is not unexpected. Indeed, we expect CASSCF(2e,3o) to underestimate the barrier because it includes the correlation of two pairing electrons while omitting correlation from other electrons, e.g., the van der Waals interactions, between π-electrons in Å-stacking of arometics. It is worth noting that, in the area of the pull-out distances of 2−3 Å, the S−T gap decreases to almost zero, from the almost net zero overlap between the two singly occupied orbitals. The small orbital overlap found for these geometries is not a result of the spatial separation as is the case when the middle BIPY$^{\bullet+}$ is pulled out for more than 5 Å but rather because the nodal structure of the orbitals results in positive and negative contributions to the overlap integral and cancel out.

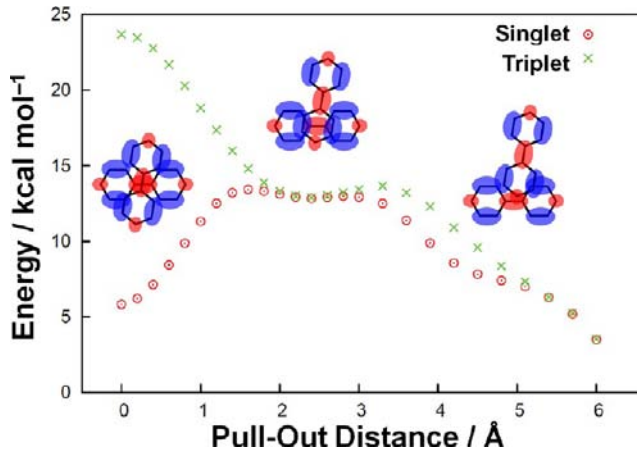

Figure 9. Singlet and triplet energy for the pull-out of the MV$^{\bullet+}$ guest of the bisradical tetracationic CBPQT$^{(\bullet+)(2+)}$ ⊂ MV$^{\bullet+}$ inclusion complex. The red and blue shading represents the phase of the singly occupied orbitals of the two BIPY$^{\bullet+}$ radical cation units. At pull-out distances of 2−3 Å, the overlap between singly occupied orbitals has both negative (overlap between red and blue) and positive (overlap between the same color) contributions, making the overall overlap integral small, leading to an almost zero S−T gap.

CONCLUSIONS

We have characterized by variable scan-rate CV the dynamic behavior of two bistable [2]rotaxanes, a [2]catenane, and one tristable [2]rotaxane, all containing a BIPY^{2+} unit which on reduction serves as a radically enhanced recognition site for the CBPQT^{4+} ring. Once the trisradical RSCC has been formed in the two bistable rotaxanes, the bistable [2]catenane, and the tristable rotaxane, a one-electron oxidation of the weakly interacting BIPY$^{\bullet+}$ radical cation to its BIPY^{2+} dication results in the formation of a bisradical state coconformation which undergoes shuttling to a bisradical donor state coconformation. In the case of the bistable [2]rotaxanes and [2]catenane, shuttling onto the adjacent electron-rich unit, TTF or DNP, occurs. We have shown that the shuttling of the bisradical state coconformation onto the TTF unit occurs faster than relaxation onto the DNP unit. The difference in the barriers governing these relaxation processes is 1.9 kcal mol^{-1}, a value which is approximately equal to the difference in the binding energy for the corresponding TTF- and DNP-containing [2]-pseudorotaxanes with the CBPQT^{4+} ring, respectively. We hypothesize that the height of the free energy barrier is dictated by the relative affinity of the adjacent π-electron rich unit, such that the stronger the recognition, the faster the shuttling and the smaller the barrier. In the case of the tristable [2]rotaxane, there is strong evidence that the ring relaxes preferentially onto the more electron-rich TTF unit in preference to the DNP one. These results have opened up the possibility of restoring the GSCC from the MSCC through the RSCC by using either (i) the TSCC reoxidation pathway, (ii) the BRCC reoxidation pathway, or (iii) a thermally assisted pathway, demonstrating a working design principle for the realization of molecular flash memory devices by employing a rotaxane which makes use of electrostatic barriers in combination with tristability.

EXPERIMENTAL SECTION

The [2]catenane **C1**·6PF$_6$[22] and the [2]rotaxanes **R1**·6PF$_6$,[17h] **R2**·6PF$_6$[17h], and **R3**·6PF$_6$[17h] were all synthesized according to previously reported procedures, and the purities of each compound were confirmed by ^{1}H NMR spectroscopy.

ASSOCIATED CONTENT

Supporting Information

For general methods, further electrochemical and NMR spectroscopic characterization. This material is available free of charge via the Internet at http://pubs.acs.org.

AUTHOR INFORMATION

Corresponding Author

stoddart@northwestern.edu

Notes

The authors declare no competing financial interest.

■ ACKNOWLEDGMENTS

We acknowledge the multidisciplinary Research Program of the University Research Initiative (MURI) award FA9550-07-1-0534 on "Bioinspired Supramolecular Enzymatic Systems" as well as the National Science Foundation (NSF) for their award CHE-0924620. We also acknowledge support from the Microelectronics Advanced Research Corporation (MARCO) and its Focus Center Research Program (FCRP) on Functional Engineered NanoArchitectonics (FENA) as well as from the Non-Equilibrium Energy Research Centre (NERC), which is an Energy Frontier Research Centre (EFRC) funded by the U.S. Department of Energy, Office of Basic Sciences (DOE-BES) under award DE-SC0000989. The research at Northwestern University (NU) was enabled by the National Center for Nano Technology Research at the King Abdulaziz City for Science and Technology (KACST) in Saudi Arabia. The authors thank Dr. Turki S. Al-Saud and Dr. Mohamed B. Alfageeh at KACST for their generous support of this research. A.C.F, D.C., W.A.G., and J.F.S. were all beneficiaries of the WCU Program (NRF R-31-2008-000-10055-0) funded by the Ministry of Education, Science and Technology, Korea. A.C.F. and D.C. acknowledge support from NSF Graduate Research Fellowships.

■ REFERENCES

(1) (a) Flood, A. H.; Stoddart, J. F.; Steuerman, D. W.; Heath, J. R. *Science* **2004**, *06*, 2055. (b) Lu, W.; Lieber, C. M. *Nat. Mater.* **2007**, *6*, 841. (c) Silvi, S.; Venturi, M.; Credi, A. *J. Mater. Chem.* **2009**, *19*, 2279. (d) Credi, A.; Semeraro, M.; Silvi, S.; Venturi, M. *Antioxid. Redox Signaling* **2011**, *14*, 1119.

(2) Tang, C.; Sivanandan, K.; Stahl, B. C.; Fredrickson, G. H.; Kramer, E. J.; Hawker, C. J. *ACS Nano* **2010**, *4*, 285.

(3) Salaita, K.; Wang, Y.; Mirkin, C. A. *Nat. Nanotechnol.* **2007**, *2*, 145.

(4) (a) Aviram, A.; Ratner, M. A. *Chem. Phys. Lett.* **1974**, *29*, 277. (b) Joachim, C.; Ratner, M. A. *Proc. Natl. Acad. Sci. U.S.A.* **2005**, *102*, 8801. (c) Heath, J. R. *Annu. Rev. Mater. Res.* **2009**, *39*, 1. (d) van der Molen, S. J.; Liljeroth, P. *J. Phys.: Condens. Matter* **2010**, *22*, 133001.

(5) (a) Moore, A. M.; Yeganeh, S.; Yao, Y.; Claridge, S. A.; Tour, J. M.; Ratner, M. A.; Weiss, P. S. *ACS Nano* **2010**, *4*, 7630. (b) Kiguchi, M.; Takahashi, T.; Takahashi, Y.; Yamauchi, Y.; Murase, T.; Fujita, M.; Tada, T.; Watanabe, S. *Angew. Chem., Int. Ed.* **2011**, *50*, 5708. (c) Schneebeli, S. T.; Kamenetska, M.; Cheng, Z.; Skouta, R.; Friesner, R. A.; Venkataraman, L.; Breslow, R. *J. Am. Chem. Soc.* **2011**, *133*, 2136.

(6) (a) Collier, C. P.; Wong, E. W.; Bělohradský, M.; Raymo, F. M.; Stoddart, J. F.; Kuekes, P. J.; Williams, R. S.; Heath., J. R. *Science* **1999**, *285*, 391. (b) Wong, E. W.; Collier, C. P.; Bělohradský, M.; Raymo, F. M.; Stoddart, J. F.; Heath, J. R. *J. Am. Chem. Soc.* **2000**, *122*, 5831. (c) Collier, C. P.; Mattersteig, G.; Wong, E. W.; Luo, Y.; Beverly, K.; Sampaio, J.; Raymo, F. M.; Stoddart, J. F.; Heath., J. R. *Science* **2000**, *289*, 1172. (d) Collier, C. P.; Jeppesen, J. O.; Luo, Y.; Perkins, J.; Wong, E. W.; Heath, J. R.; Stoddart, J. F. *J. Am. Chem. Soc.* **2001**, *123*, 12632. (e) Luo, Y.; Collier, C. P.; Jeppesen, J. O.; Nielsen, K. A.; DeIonno, E.; Ho, G.; Perkins, J.; Tseng, H.-R.; Yamamoto, T.; Stoddart, J. F.; Heath, J. R. *Chem. Phys. Chem* **2002**, *3*, 519. (f) Green, J. E.; Choi, J. W.; Boukai, A.; Bunimovich, Y.; Johnston-Halperin, E.; DeIonno, E.; Luo, Y.; Sheriff, B. A.; Xu, K.; Shin, Y. S.; Tseng, H.-R.; Stoddart, J. F.; Heath, J. R. *Nature* **2007**, *445*, 414. (g) Zhang, W.; DeIonno, E.; Dichtel, W. R.; Fang, L.; Trabolsi, A.; Olsen, J.-C.; Benitéz, D.; Heath, J. R.; Stoddart, J. F. *J. Mater. Chem.* **2011**, *21*, 1487. (h) Coskun, A.; Banaszak, M.; Astumian, R. D.; Stoddart, J. F.; Grzybowski, B. A. *Chem. Soc. Rev.* **2012**, *41*, 19. (i) Coskun, A.; Spruell, J. M.; Barin, G.; Dichtel, W. R.; Flood, A. H.; Botros, Y. Y.; Stoddart, J. F. *Chem. Soc. Rev* **2012**, *41*, 4827.

(7) Melosh, N. A.; Boukai, A.; Diana, F.; Gerardot, B.; Badolato, A.; Petroff, P. M.; Heath, J. R. *Science* **2003**, *300*, 112.

(8) (a) Nygaard, S.; Leung, K. C-F.; Aprahamian, I.; Ikeda, T.; Saha, S.; Laursen, B. W.; Kim, S.-Y.; Hansen, S. W.; Stein, P. C.; Flood, A. H.; Stoddart, J. F.; Jeppesen, J. O. *J. Am. Chem. Soc.* **2007**, *129*, 960. (b) Aprahamian, I.; Dichtel, W. R.; Ikeda, T.; Heath, J. R.; Stoddart, J. F. *Org. Lett.* **2007**, *9*, 1287. (c) Dichtel, W. R.; Heath, J. R.; Stoddart, J. F. *Phil. Trans. R. Soc. London Ser. A* **2007**, *365*, 1607. (d) Stoddart, J. F.; Colquhoun, H. M. *Tetrahedron* **2008**, *64*, 8231. (e) Stoddart, J. F. *Chem. Soc. Rev.* **2009**, *38*, 1802. (f) Olsen, J.-C.; Fahrenbach, A. C.; Trabolsi, A.; Friedman, D. C.; Dey, S. K.; Gothard, C. M.; Shveyd, A. K.; Gasa, T. B.; Spruell, J. M.; Olson, M. A.; Wang, C.; Jacquot de Rouville, H.-P.; Botros, Y. Y.; Stoddart, J. F. *Org. Biomol. Chem.* **2011**, *9*, 7126. (g) Li, H.; Fahrenbach, A. C.; Coskun, A.; Zhu, Z.; Barin, G.; Zhao, Y.-L.; Botros, Y. Y.; Sauvage, J.-P.; Stoddart, J. F. *Angew. Chem., Int. Ed.* **2011**, *50*, 6782. (h) Dey, S. K.; Coskun, A.; Fahrenbach, A. C.; Barin, G.; Basuray, A. N.; Trabolsi, A.; Botros, Y. Y.; Stoddart, J. F. *Chem. Sci.* **2011**, *2*, 1046.

(9) (a) Odell, B.; Reddington, M. V.; Slawin, A. M. Z.; Spencer, N.; Stoddart, J. F.; Williams, D. J. *Angew. Chem., Int. Ed. Engl.* **1988**, *27*, 1547. (b) Brown, C. L.; Philp, D.; Stoddart, J. F. *Synlett* **1991**, *7*, 462. (c) Asakawa, M.; Dehaen, W.; L'abbé, G.; Menzer, S.; Nouwen, J.; Raymo, F. M.; Stoddart, J. F.; Williams, D. J. *J. Org. Chem.* **1996**, *61*, 9591. (d) Capobianchi, S.; Doddi, G.; Ercolani, G.; Keyes, J. W.; Mencarelli, P. *J. Org. Chem.* **1997**, *62*, 7015. (e) Sue, C.-H.; Basu, S.; Fahrenbach, A. C.; Shveyd, A. K.; Dey, S. K.; Botros, Y. Y.; Stoddart, J. F. *Chem. Sci.* **2010**, *1*, 119.

(10) (a) Philp, D.; Slawin, A. M. Z.; Spencer, N.; Stoddart, J. F.; Williams, D. J. *J. Chem. Soc., Chem. Commun.* **1991**, 1584. (b) Bendikov, M.; Wudl, F.; Perepichka, D. F. *Chem. Rev.* **2004**, *104*, 4891. (c) Ziganshina, A. Y.; Ko, Y. H.; Jeon, W. S.; Kim, K. *Chem. Commun.* **2004**, 806. (d) Yoshizawa, M.; Kumazawa, K.; Fujita, M. *J. Am. Chem. Soc.* **2005**, *127*, 13456. (e) Canevet, D.; Sallé, M.; Zhang, G.; Zhang, D.; Zhu, D. *Chem. Commun.* **2009**, *17*, 2245. (f) Spruell, J. M.; Coskun, A.; Friedman, D. C.; Forgan, R. S.; Sarjeant, A. A.; Trabolsi, A.; Fahrenbach, A. C.; Barin, G.; Paxton, W. F.; Dey, S. K.; Olson, M. A.; Benítez, D.; Tkatchouk, E.; Colvin, M. T.; Carmielli, R.; Caldwell, S. T.; Rosair, G. M.; Hewage, S. G.; Duclairoir, F.; Seymour, J. L.; Slawin, A. M. Z.; Goddard, W. A., III; Wasielewski, M. R.; Cooke, G.; Stoddart, J. F. *Nat. Chem.* **2010**, *2*, 870. (g) Coskun, A.; Spruell, J. M.; Barin, G.; Fahrenbach, A. C.; Forgan, R. S.; Colvin, M. T.; Carmielli, R.; Benítez, D.; Tkatchouk, E.; Friedman, D. C.; Sarjeant, A. A.; Wasielewski, M. R.; Goddard, W. A., III; Stoddart, J. F. *J. Am. Chem. Soc.* **2011**, *133*, 4538. (h) Hansen, S. W.; Stein, P. C.; Sørensen, A.; Share, A. I.; Witlicki, E. H.; Kongsted, J.; Flood, A. H.; Jeppesen, J. O. *J. Am. Chem. Soc.* **2012**, *134*, 3857.

(11) (a) Steuerman, D. W.; Tseng, H.-R.; Peters, A. J.; Flood, A. H.; Jeppesen, J. O.; Nielsen, K. A.; Stoddart, J. F.; Heath, J. R. *Angew. Chem., Int. Ed.* **2004**, *43*, 6486. (b) Flood, A. H.; Peters, A. J.; Vignon, S. A.; Steuerman, D. W.; Tseng, H.-R.; Kang, S.; Heath, J. R.; Stoddart, J. F. *Chem.—Eur. J.* **2004**, *10*, 6558. (c) Choi, J. W.; Flood, A. H.; Steuerman, D. W.; Nygaard, S.; Braunschweig, A. B.; Moonen, N. N. P.; Laursen, B. W.; Luo, Y.; Delonno, E.; Peters, A. J.; Jeppesen, J. O.; Xe, K.; Stoddart, J. F.; Heath, J. R. *Chem.—Eur. J.* **2006**, *12*, 261.

(12) Vignon, S. A.; Stoddart, J. F. *Collect. Czech. Chem. Commun.* **2005**, *70*, 1493.

(13) (a) Jeppesen, J. O.; Nielsen, K. A.; Perkins, J.; Vignon, S. A.; Di Fabio, A.; Ballardini, R.; Gandolfi, M. T.; Venturi, M.; Balzani, V.; Becher, J.; Stoddart, J. F. *Chem.—Eur. J.* **2003**, *9*, 2982. (b) Jeppesen, J. O.; Vignon, S. A.; Stoddart, J. F. *Chem.—Eur. J.* **2003**, *9*, 4611. (c) Kang, S.; Vignon, S. A.; Tseng, H.-R.; Stoddart, J. F. *Chem.—Eur. J.* **2004**, *10*, 2555. (d) Jeppesen, J. O.; Nygaard, S.; Vignon, S. A.; Stoddart, J. F. *Eur. J. Org. Chem.* **2005**, *1*, 196. (e) Coskun, A.; Friedman, D. C.; Li, H.; Patel, K.; Khatib, H. A.; Stoddart, J. F. *J. Am. Chem. Soc.* **2009**, *131*, 2493. (f) Zhang, K.-D.; Zhou, X.; Wang, G.-T.; Liu, Y.; Zhang, Y.; Lu, H.-J.; Jiang, X.-K.; Li, Z.-T. *Angew. Chem. Int. Ed.* **2011**, *50*, 9866. (g) Avellini, T.; Li, H.; Coskun, A.; Barin, G.; Trabolsi, A.; Basuray, A. N.; Dey, S. K.; Credi, A.; Silvi, S.; Stoddart, J. F.; Venturi, M. *Angew. Chem., Int. Ed.* **2012**, *51*, 1611.

(14) (a) Ghosh, P.; Federwisch, G.; Kogej, M.; Schalley, C. A.; Haase, D.; Saak, W.; Lützen, A.; Gschwind, R. M. *Org. Biomol. Chem.* **2005**, *3*, 2691. (b) Brough, B.; Northrop, B. H.; Schmidt, J. J.; Tseng, H.-R.; Houk, K. N.; Stoddart, J. F.; Ho, C.-M. *Proc. Natl. Acad. Sci. U.S.A.* **2006**, *103*, 8583. (c) Trabolsi, A.; Fahrenbach, A. C.; Dey, S. K.; Share, A. I.; Friedman, D. C.; Basu, S.; Gasa, T. B.; Khashab, N. M.; Saha, S.; Aprahamian, I.; Khatib, H. A.; Flood, A. H.; Stoddart, J. F. *Chem. Commun.* **2010**, *46*, 871. (d) Li, H.; Zhao, Y.-L.; Fahrenbach, A. C.; Kim, S.-Y.; Paxton, W. F.; Stoddart, J. F. *Org. Biomol. Chem.* **2011**, *9*, 2240. (e) Hmadeh, M.; Fahrenbach, A. C.; Basu, S.; Trabolsi, A.; Benítez, D.; Li, H.; Albrecht-Gary, A.-M.; Elhabiri, M.; Stoddart, J. F. *Chem.—Eur. J.* **2011**, *17*, 6076.

(15) (a) Nakahara, A.; Wang, J. H. *J. Phys. Chem.* **1963**, *67*, 496. (b) Allwood, B. L.; Shahriari-Zaverah, H.; Stoddart, J. F.; Williams, D. J. *J. Chem. Soc., Chem. Commun.* **1987**, 1058. (c) Ashton, P. R.; Chrystal, E. J. T.; Mathias, J. P.; Parry, K. P.; Slawin, A. M. Z.; Spencer, N.; Stoddart, J. F.; Williams, D. J. *Tetrahedron Lett.* **1987**, *28*, 6367. (d) Odell, B.; Reddington, M. V.; Slawin, A. M. Z.; Spencer, N.; Stoddart, J. F.; Williams, D. J. *Angew. Chem., Int. Ed. Engl.* **1988**, *27*, 1547. (e) Asakawa, M.; Dehaen, W.; L'abbé, G.; Menzer, S.; Nouwen, J.; Raymo, F. M.; Stoddart, J. F.; Williams, D. J. *J. Org. Chem.* **1996**, *61*, 9591. (f) Monk, P. M. S.; Hodgkinson, N. M.; Partridge, R. D. *Dyes Pigm.* **1999**, *43*, 241. (g) Chiang, P.-T.; Cheng, P.-N.; Lin, C.-F.; Liu, Y.-H.; Lai, C.-C.; Peng, S.-M.; Chiu, S.-H. *Chem.—Eur. J.* **2006**, *12*, 865. (h) Gasa, T. B.; Spruell, J. M.; Dichtel, W. R.; Sørensen, T. J.; Philp, D.; Stoddart, J. F.; Kuzmič, P. *Chem.—Eur. J.* **2009**, *15*, 106. (i) Iordache, A.; Oltean, M.; Milet, A.; Thomas, F.; Baptiste, B.; Saint-Aman, E.; Bucher., C. *J. Am. Chem. Soc.* **2012**, *134*, 2653. (j) Freitag, M.; Gundlach, L.; Piotrowiak, P.; Galoppini, E. *J. Am. Chem. Soc.* **2012**, *134*, 3358.

(16) Scott, J. C.; Bozano, L. D. *Adv. Mater.* **2007**, *19*, 1452.

(17) (a) Michaelis, L.; Hill, E. S. *J. Gen. Physiol.* **1933**, *16*, 859. (b) Michaelis, L. *Chem. Rev.* **1935**, *16*, 243. (c) Kosower, E. M.; Cotter, J. L. *J. Am. Chem. Soc.* **1964**, *86*, 5524. (d) Bird, C. L.; Kuhn, A. T. *Chem. Soc. Rev.* **1981**, *10*, 49. (e) Monk, P. M. S. *The Viologens: Physicochemical Properties, Synthesis and Applications of the Salts of 4,4′-Bipyridine*; Wiley: New York, 1998. (f) Park, J. W.; Choi, N. H.; Kim, J. H. *J. Phys. Chem.* **1996**, *100*, 769. (g) Jeon, W. S.; Kim, H.-J.; Lee, C.; Kim, K. *Chem. Commun.* **2002**, 1828. (h) Trabolsi, A.; Khashab, N.; Fahrenbach, A. C.; Friedman, D. C.; Colvin, M. T.; Cotí, K. K.; Benítez, D.; Tkatchouk, E.; Olsen, J.-C.; Belowich, M. E.; Carmielli, R.; Khatib, H. A.; Goddard, W. A., III; Wasielewski, M. R.; Stoddart, J. F. *Nat. Chem.* **2010**, *2*, 42. (i) Li, H.; Fahrenbach, A. C.; Dey, S. K.; Basu, S.; Trabolsi, A.; Zhu, Z.; Botros, Y. Y.; Stoddart, J. F. *Angew. Chem., Int. Ed.* **2010**, *49*, 8260. (j) Fahrenbach, A. C.; Barnes, J. C.; Lanfranchi, D. A.; Li, H.; Coskun, A.; Gassensmith, J. J.; Liu, Z.; Benítez, D.; Trabolsi, A.; Goddard, W. A.; Elhabiri, M.; Stoddart, J. F. *J. Am. Chem. Soc.* **2012**, *134*, 3061.

(18) Coskun, A.; Banaszak, M.; Astumian, R. D.; Stoddart, J. F.; Grzybowski, B. A. *Chem. Soc. Rev.* **2012**, *41*, 19.

(19) (a) Katz, E.; Lioubashevsky, O.; Willner, I. *J. Am. Chem. Soc.* **2004**, *126*, 15520. (b) Katz, E.; Baron, R.; Willner, I.; Richke, N.; Levine, R. D. *ChemPhysChem* **2005**, *6*, 2179.

(20) Kim, H.; Goddard, W. A., III; Jang, S. S.; Dichtel, W. R.; Heath, J. R.; Stoddart, J. F. *J. Phys. Chem. A* **2009**, *113*, 2136.

(21) It is important to note that this barrier of 19 kcal mol^{-1}, which corresponds to a half-life of *ca.* 1 min, was measured in the presence of 0.1 M TBA·PF_6; a necessity when it comes to performing CV experiments. As a signature of the fact that the increase in the barrier is caused by electrostatics, in the absence of the TBA·PF_6 electrolyte, which screens electrostatic repulsions, we have observed the half-life of the MSCC to be much longer, i.e., on the order of days.

(22) Zhu, Z.; Fahrenbach, A. C.; Li, H.; Barnes, J. C.; Liu, Z.; Dyar, S. M.; Zhang, H.; Lei, J.; Carmieli, R.; Sarjeant, A. A.; Stern, C. L.; Wasielewski, M. R.; Stoddart, J. F. *J. Am. Chem. Soc.* **2012**, *134*, 11709.

(23) We have observed a similar interplay between competing donor−acceptor interactions and radical−radical interactions, see refs 10f and g. It is important to note that no such variable scan-rate-dependent behavior is observed in the case of a rotaxane containing only a $BIPY^{2+}$ recognition unit with no accompanying π-electron-rich unit in the dumbbell component; see ref 17j.

(24) Kaifer, A. E.; Gómez-Kaifer, M. *Supramolecular Electrochemistry*, Wiley-VCH, New York, 1999.

(25) From the Pauli exclusion principle, we can reason that the only way for the two spin-paired electrons to unpair is for one electron to make the transition into a LUMO, since no two electrons can occupy the exact same quantum state. Although there is somewhat of an ongoing debate in the literature about the exact nature of the electronic transitions resulting from the observed absorption bands for dimerized $BIPY^{\bullet+}$ radical cations, the absorption band typically observed in the NIR region most likely involves the transition of one of the spin-paired radical electrons into a higher energy orbital, thus allowing unpairing of the spins to occur into a triplet state. If we make the assumption that the energy of this near-IR transition is roughly equal to the reorganizational energy for the electronic transfer to occur, employing the near-IR absorption band (1075 nm, ref 17h) of a previously reported trisradical complex as a model system, we can calculate a reorganizational energy of approximately 26 kcal mol^{-1}; a value which is reasonably consistent with our theoretical calculations which predict that approximately 9 kcal mol^{-1} of energy is needed to unpair the spins of the radical electrons from a singlet to a triplet state. For more details, see: Lü, J.-M.; Rosokha, S. V.; Kochi, J. K. *J. Am. Chem. Soc.* **2003**, *125*, 12161.

(26) Fahrenbach, A. C.; Barnes, J. C.; Li, H.; Benítez, D.; Basuray, A. N.; Fang, L.; Sue, C.-H.; Barin, G.; Dey, S. K.; Goddard, W. A., III.; Stoddart, J. F. *Proc. Natl. Acad. Sci. U.S.A.* **2011**, *108*, 20416.

(27) Balzani, V.; Credi, A.; Mattersteig, G.; Matthews, O. A.; Raymo, F. M.; Stoddart, J. F.; Venturi, M.; White, A. J. P.; Williams, D. J. *J. Org. Chem.* **2000**, *65*, 1924.

(28) Crystal data for $\mathbf{C1}^{2(\bullet+)(2+)}\cdot 4PF_6$: $C_{92}H_{108}F_{24}N_{16}O_9P_4$, M_r = 2169.33, triclinic, $P\bar{1}$, a = 15.2916(13), b = 26.090(2), c = 26.927(3) Å, α = 103.784(6)°, β = 90.188(6)°, γ = 99.938(5)°, V = 10265.7 $Å^3$, T = 100(2) K, Z = 4, D_c = 1.404 g cm^{-3}, μ(Cu-Kα) 1.613 mm^{-1}, $F(000)$ = 4496. Independent measured reflections 20 948. R_1 = 0.1049, wR_2 = 0.2713 for 10 743 independent observed reflections [$2\theta \leq 100.86°$, $I > 2\sigma(I)$] CCDC 887663.

(29) Hunter, C. A.; Sanders, J. K. M. *J. Am. Chem. Soc.* **1990**, *112*, 5525.

(30) Fang, L.; Basu, S.; Sue, C.-H.; Fahrenbach, A. C.; Stoddart, J. F. *J. Am. Chem. Soc.* **2011**, *133*, 396.

(31) Bockman, T. M.; Kochi, J. K. *J. Org. Chem.* **1990**, *55*, 4127.

(32) This observed effect caused by population of anitbonding orbitals which is caused by either total electron transfer of radical electrons or partial charge transfer from donor−acceptor interactions is not limited to the case of $BIPY^{2+}$ units. A whole range of redox-active species categorized as a class of molecules called by S. Hünig as the "violenes", i.e., any molecular framework containing at least two heteroatoms separated by a conjugated network of carbon atoms, are observed to undergo similar transformations in their bonding structure. For more details on violenes, see: Hünig, S. *Pure Appl. Chem.* **1967**, *15*, 109. For a specific example detailing the effects of donor−acceptor interactions on the bonding structure of a TTF^{2+} dication, see: Ashton, P. R.; Balzani, V.; Becher, J.; Credi, A.; Fyfe, M. C. T.; Mattersteig, G.; Menzer, S.; Nielsen, M. B.; Raymo, F. M.; Stoddart, J. F.; Venturi, M.; Williams, D. J. *J. Am. Chem. Soc.* **1999**, *121*, 3951.

(33) Witlicki, E. H.; Johnsen, C.; Hansen, S. W.; Silverstein, D. W.; Bottomley, V. J.; Jeppesen, J. O.; Wong, E. W.; Jensen, L.; Flood, A. H. *J. Am. Chem. Soc.* **2011**, *133*, 7288.

(34) Basu, S; Coskun, A.; Friedman, D. C.; Olson, M. A.; Benítez, D.; Tkachouk, E.; Barin, G.; Young, J.; Fahrenbach, A. C.; Goddard, W. A., III; Stoddart, J. F. *Chem.—Eur. J.* **2011**, *17*, 2107.

(35) (a) Jørgensen, T.; Hansen, T. K.; Becher, J. *Chem. Soc. Rev.* **1994**, *23*, 41. (b) Spruell, J. M.; Paxton, W. F.; Olsen, J.-C.; Benítez, D.; Tkatchouk, E.; Stern, C. L.; Trabolsi, A.; Friedman, D. C.; Goddard, W. A., III; Stoddart, J. F. *J. Am. Chem. Soc.* **2009**, *131*, 11571.